Final Report:
Massachusetts Bay Dye Study

Massachusetts Water Resources Authority

Environmental Quality Department
Report 1994-17

Citation:

Geyer WR, Ledwell JR. 1994. Final Report: Massachusetts Bay Dye Study. Boston: Massachusetts Water Resources Authority. Report ENQUAD 1994-17. 39 p.

BACK OF FRONT COVER

Final Report:
Massachusetts Bay Dye Study

W. Rockwell Geyer and James R. Ledwell
Department of Applied Ocean Physics and Engineering
Woods Hole Oceanographic Institution
Woods Hole, MA 02543

Submitted to:

Massachusetts Water Resources Authority
Charleston Navy Yard
39 First Ave.
Boston, MA 02129

September 6, 1994

Summary

A dye experiment was performed in Massachusetts Bay during August 1993, to determine the rates of vertical and horizontal dispersion. Rhodamine dye was released as a thin patch in the thermocline of western Massachusetts Bay, and the vertical and horizontal distributions of the dye were monitored for four days following the release using a ship-deployed fluorometer. Measurements of water properties, current velocity and winds were also obtained during the deployment. The vertical scale of the patch increased slowly during the observations, with a nearly Gaussian distribution. Vertical diffusivity during the period was 0.04–0.08 $cm^2\ s^{-1}$. The horizontal spreading of the patch was roughly isotropic for the first two days, but then it started to elongate in the N–S direction. The horizontal dispersion coefficient was 3 $m^2\ s^{-1}$ for the first two days, increasing to 16 $m^2\ s^{-1}$ between the 4th and 5th day, apparently as a result of increased mean shear.

The stratification and shear for the period were typical of summertime conditions, based on comparisons with data from previous years. Tidal range increased to spring tide conditions during the experiment. Winds were southeasterly to northeasterly, with average speeds of 4 m s^{-1}, in contrast to southwesterly winds of similar magnitude typical of this season. Based on these environmental variables, the factors influencing vertical dispersion were typical of summertime conditions, perhaps slightly more energetic than average due to the spring tide conditions. However, the vertical mixing rate appears to be roughly half of the integral estimate based on seasonal variation of temperature and salinity in Massachusetts Bay. The most likely explanation for the discrepancy is that more intense mixing and advective exchange occurs in the boundary region where the thermocline intersects the bottom.

1 Introduction

The rate of vertical mixing in Massachusetts Bay is an important physical parameter with respect to the impact of the new sewage outfall. Nutrients tend to be depleted in surface waters due to uptake by phytoplankton, but there are generally high nutrient concentrations below the seasonal thermocline due to regeneration. The rate at which nutrients are transported back into the surface waters by mixing is an important factor controlling the rate of primary production in the euphotic zone. The observations by Townsend et al., 1990 indicate that much of the surface waters of Massachusetts Bay are depleted in nutrients during the summer months; only the region close to Boston Harbor that receives the input from Boston's sewage outfalls shows significant nutrient concentrations in surface waters. The discharge from the new sewage outfall will be trapped within the thermocline during the stratified portion of the annual cycle, but vertical mixing will provide a mechanism for transport into the euphotic zone.

Moreover, the horizontal transport of effluent away from western Massachusetts Bay controls the build-up of nutrients and contaminants in the water column. Current observations near the new outfall indicate that the mean velocity is weak, thus the exchange with the rest of Massachusetts Bay is accomplished by horizontal dispersion due to fluctuating currents. Little is known in general about the rate of horizontal dispersion within the pycnocline in coastal waters. Numerical models cannot accurately address the problem, due to the importance of motions at scales smaller the typical grid resolution (e.g., Blumberg et al., 1993).

A means of addressing both the rate of vertical mixing and horizontal dispersion is a controlled dye release. A dye release experiment was performed over a five-day period in the summer of 1993 to quantify the rate of vertical mixing and horizontal dispersion during summertime conditions. The vertical and horizontal distributions of dye were measured over the four days following the release to quantify the rates of vertical mixing and horizontal dispersion within the thermocline. Measurements of shear and stratification within the thermocline provided estimates of the forcing variables, providing a means of generalizing the results from this four-day period to the climatological conditions of the bay.

2 Methods

The dye study was in western Massachusetts Bay, near the site of the new Boston sewage outfall (Fig. 1). Dye injection took place on August 16, 1993, and the dye patch was surveyed immediately following the injection and for four days following the release.

2.1 Dye Injection

The dye was injected by pumping from drums on the deck of R/V Asterias to the target density surface through a hose with a nozzle at the end, mounted on an injection "sled". The tow speed during injection was 1 knot, the wake of the sled adding to the effect of the nozzle in attaining an initial dispersion and dilution of the dye. Also mounted on the sled was a SeaBird 9/11 CTD whose output was used by the winch operator to maintain the sled as close as possible to the target density surface. Noise in the salinity calculated from the CTD signal was greater than the natural variability at constant density, so temperature was used as a surrogate for potential density in guiding the injection. The target temperature was 12.5° C. The dye pump turned off automatically when the temperature was more than 0.5° away from this target, equivalent to 0.8 m in the mean gradient. Control of the sled was accurate enough that departures this large rarely occurred, however.

The total amount of Rhodamine-WT injected was approximately 55 kg. The dye was procured as an aqueous solution of 20% dye, by weight. 275 kg of this solution was mixed with methanol in a ratio of approximately 5/2 to bring the specific gravity to 1.022 (at 27° C).

It was learned in the laboratory that the specific gravity of the mixture depended rather strongly on temperature. It was also learned that when the mixture was gently injected into a cylinder of seawater the density of the dyed filaments seemed to increase with time, indicating that the methanol was preferentially diffusing away. These phenomena must be taken into account when the goal is to tag water of a very specific density, as in the present experiment.

The dye pumping system was simple, but effective. The central element was a gear pump on deck, in parallel with a bypass valve, used to adjust the flow. The maximum flow, with the bypass valve closed was 8 liters/min. The flow used for the injection was 5 liters/min.

The dye was injected as two intersecting horizontal lines, approximately 2 km long. Satellite tracked "ARGOS" drifters were deployed at even intervals during

the dye injection. The drifters had 5-m long, "holey sock" drogues, 1-m in diameter, centered at 10-m depth, which was the average depth of the 12.5° surface during the deployment day (Fig. 2). The drifters allowed the horizontal motions of the dye patch to be estimated for guiding the surveying effort.

2.2 Dye Sampling

The dye was sampled with a system built around the SeaBird 9/11 CTD on a sampling frame, heavily weighted and operated in tow-yo mode at lateral speeds of 1.0 to 1.5 m/s and vertical speeds of 0.3 to 0.7 m/s. Two Chelsea Instruments fluorometers were incorporated in the system, one set up for Rhodamine, and the other set up for Chlorophyll. There were also 2 auxiliary temperature sensors, one 1.60 m above the primary sensor, and the other 0.75 m below.

The minimum detectable level of Rhodamine by the fluorometer in clear water is approximately 0.01 ppb (parts per billion by weight). However, a false signal was obtained in parts of the water column in Massachusetts Bay which was correlated with the chlorophyll signal. Some of the false signal could therefore be removed by taking this correlation into account. The resulting rms noise in the dye signal was approximately 0.02 ppb, and systematic errors in the region of the dye patch are also estimated to be about 0.02 ppb.

The flash rate (equivalent to the initial sampling rate) of the fluorometers was 5.5 hz. However, various filters in the instrument reduce the effective sampling rate to 1 hz, and also introduce a lag of approximately 1.5 seconds. This means that the raw dye signal lags behind the CTD measurements by this amount of time. This lag is common to all fluorometers currently on the market, and is not included in the manufacturers' specifications. It can create serious mismatch between the CTD measurements and the dye signal when profiling in stratified waters. We learned about this lag the from the actual field data and alert future investigators to the problem. We handled it as accurately as possible by incorporating the lag in post-processing of the CTD/dye data, adjusting the lag to maximize the correlation between adjacent up and down casts of the tow-yos.

3 Results

3.1 Vertical Mixing

Vertical mixing as well as horizontal spreading resulted in a rapid reduction in dye concentration with time. The decrease in concentration within the patch is evident in the daily average dye profiles (Fig. 3). Although the vertical axis is depth, the averaging was done at levels of constant temperature to remove the influence of internal waves, and then the mean temperature profile was used to convert back to depth coordinates. The irregular structure of the patch during day 1 is due to a small number of profiles within the dye patch. Likewise, the non-Gaussian shape of the profile during Day 2 is due to a limited number of profiles in the most concentrated portion of the patch. The profiles become much smoother on subsequent days, as the patch becomes spatially distributed and a larger number of profiles are obtained in the core of the patch. It is difficult in this figure to quantify the vertical spreading of the patch, but it is clear that its vertical spreading is small in comparison with the decrease in concentration. This decrease is due mostly to the horizontal spreading of the dye (see the following subsection).

The most comprehensive surveys of the dye patch were performed on days 3 and 5, and so these provide the most accurate assessment of the vertical diffusivity. Figure 4 shows normalized concentration profiles from Days 3 and 5, indicating the increase in vertical extent of the patch on Day 5. This modest increase in the thickness of the dye patch is adequate to obtain an estimate of the diffusivity. The vertical spreading of the patch was quantified by fitting a Gaussian to each of the observed profiles. The diffusivity is then obtained by the relation

$$K_z = \frac{1}{2}\frac{d\sigma^2}{dt}$$

where K_z is the vertical diffusivity, σ^2 is the second moment of the vertical dye distribution (2.55σ is roughly the thickness of the patch), and d/dt is the normal time derivative. The change in patch thickness with time is shown graphically in Fig. 5. When extrapolated back to t=0, it yields an initial patch thickness of slightly less than 1 m, which is consistent with the limited estimates of the initial conditions. Given the uncertainty of the initial conditions, these values yield an estimate of $K_z = 0.04 - 0.08$ cm^2 s^{-1}. The upper limit of the estimate is quite firm, since it is based on growth from an infinitesimally thin layer on Day 1 to the well-sampled distribution on Day 5.

3.2 Horizontal Stirring and Mixing

3.2.1 Horizontal Spreading

An overall indication of the horizontal spreading of the dye patch is shown in Fig. 6. The trajectory of the dye release is indicated (day 1), and the outline of the patch is indicated for successive survey days, indicated by the concentration contour that is roughly one third the maximum value for that day. The patch slowly moved to the northwest during the five-day period (average speed 1.3 cm s^{-1}). Between Day 1 and 2, it spread approximately uniformly in the east–west (E–W) and north–south (N–S) directions, after which it began elongating in the N–S direction.

Detailed contour plots of the horizontal dye distributions during successive days are shown on Fig. 7. To correct for the apparent distortion of the patch due to tidal motions during each survey (tidal excursion distance is approximately 2 km), a Lagrangian reference frame was adopted, so that the coordinates are defined with respect to a point that moves with the water motion at 10-m depth. The water motion was determined with the shipboard ADCP rather than the drifters, as the ADCP was determined to be more accurate based on comparison with the dye trajectory. The spacing between the survey lines was too great to provide a precise map of the spatial distribution, but the along-track variation provides an indication of the scales of variability of the dye. During days 4 and 5 the patch exhibits a number of local maxima; these may have been discrete blobs as indicated on the contour plots or elongated streaks. A finer scale survey would be required to distinguish between these possibilities.

The E–W and N–S integrated dye distributions (Fig. 8) provide a means of assessing the nature and rate of horizontal spreading of the dye. Some of the distributions appear Gaussian, suggesting uniform horizontal mixing, while others deviate markedly from a Gaussian shape and indicate a more complex dispersion process. Nevertheless, the temporal increase in the spatial scales of the patch can be used to obtain a rough estimate of the horizontal dispersion rate. Table 1 summarizes the results of this analysis. The dispersion rate based on the observed spreading rate increases monotonically from 3.1 m^2 s^{-1} to 16.4 m^2 s^{-1} during the 5 day period. There is possibly a systematic error in these results due to some unsurveyed fraction of dye during days 4 and 5, which would increase the moments. Another estimate of the dispersion was obtained by normalizing the estimates of σ based on the integrated mass of dye, to correct for the unresolved fraction. This is equivalent to using the observed decline in concentration with time to obtain a diffusivity estimate. This approach yields similar numbers to the previous one, but it shows a marked increase in diffusivity between days 3 and 4. This increase in

diffusivity is associated with the N–S stretching of the patch, which is most notable during days 4 and 5.

The mass of dye was estimated each day from the calculated distributions. Of the 55 kg of dye that were deployed, the estimates based on the surveys were as follows: day 2– 111 kg; day 3– 75 kg; day 4– 36 kg; day 5– 54 kg. The large discrepancy for day 2 is attributed to the limited spatial sampling, but the overestimate for day 3 is harder to explain. It is also likely, based on the extent of the distributions during days 4 and 5, that these are underestimates, which would bring them into line with the day 3 estimate. Thus it appears that there was a systematic error in calibration that lead to an overestimate of the total dye concentration. Although this adversely impacts the mass balance calculations, it does not affect the estimates of horizontal and vertical moments for diffusion calculations.

3.2.2 Decline of Patchiness

The horizontal spreading of the dye does not necessarily imply mixing; in the absence of small-scale mixing processes the patch may be distorted and stretched, but retain intact blobs or streaks of unmixed fluid. A means of assessing the degree of mixing is to document the time-variation of the maximum dye concentration within the patch.

The concentration of dye in the mixture coming out of the injection nozzle was 14% by weight. This mixture was immediately diluted into the wake of the injection system, which was towed at 0.5 m/s. The rms vertical spread of the initial plume was about 0.9 m, estimated from the subsequent dispersion (Fig. 5). Experience with previous field experiments, guided by laboratory studies of wakes in stratified fluids (Lin and Pao, 1979), indicate that the rms width of the wake after a few minutes would be at least 5 times the rms vertical spread. From these estimates it can be inferred that the concentration in the a few minutes after injection would be less than 1000 ppb (parts per billion by weight).

The wake seemed to continue to spread laterally with time. Sampling approximately 4 hours after the midpoint of the injection revealed the rms width of the streaks to be on the order of 60 m, with a maximum concentration of 160 ppb. One day after the injection the maximum concentration found had fallen to 7 ppb. This dilution of a factor of more than 20 occurred primarily by the smearing of the initial streaks into a rather uniform patch (Fig. 7a), with a rms lateral length spread of 1000 m, just twice as large as the rms spread of the initial streaks (Table 1). Further decrease of the peak concentration had to occur by lateral and vertical spreading of the rather homogeneous patch. Thus, the dilution of the peak concen-

tration from 1 day after injection to 4 days after was just a factor of 7, down to 1 ppb (Fig. 9).

In summary, smearing of 10 to 100-m hot spots of tracer to rather homogeneous patches 1000 m across required just 24 hours, reducing peak concentrations by a factor of 20. Dilution over the next 3 days was a factor of 7 as the area of the overall patch grew by a similar factor. The final length scale of the patch was 2000 to 4000 m (Table 1). The evolution of the patchiness at larger scales will require the use of more sensitive tracers.

3.3 Environmental Data

3.3.1 Winds and Currents

The winds measured at the Boston meteorological buoy (0.5 km from the release location) during the period of the dye release experiment were generally from the SE and NE, which differs from the typical SW and NW wind regime (Fig. 10). Wind speeds were close to the climatological average for the summer. Currents measured at the same location (courtesy of U.S. Geological Survey) at 5-m depth showed weak non-tidal flows for most of the experiment (Fig. 11). A northwestward flow of 12 cm s^{-1} occurred during Day 1, but the velocity subsided to several cm s^{-1} for the remainder of the period. Tidal amplitude was increasing from intermediate to spring tides during the deployment period (Fig. 12), but the currents at 5-m showed an irregular tidal signal with no evidence of an increasing amplitude (Fig. 13). Tidal velocities were mostly in the E–W direction, with amplitudes of 10–20 cm s^{-1}.

Shipboard ADCP observations provided resolution of the currents through most of the water column (3–25 m). From these data, the barotropic (vertically averaged) and baroclinic (vertically varying) tidal motions could be distinguished. In contrast to the moored data at 5-m depth, the ADCP data indicate a steadily increasing barotropic velocity during the dye study (Fig. 14). The baroclinic component of motion was roughly half of the barotropic part, with typical amplitudes of 5–7 cm s^{-1}. The vertical structure of the baroclinic tidal velocity is indicated in Fig. 15. There was a velocity reversal close to 10-m depth, and a local extremum around 15–20-m. The vertical structure of the internal tide varied somewhat from day to day, but there were large (up to 90°) changes in its phase and orientation. These variations in internal tidal motion explain the irregular tidal velocities observed at the 5-m mooring.

3.3.2 Shear and Stratification

The stability of the water column with respect to vertical mixing depends on the relative magnitude of the shear and stratification. Buoyancy frequency

$$N = \left(-\frac{g}{\rho} \frac{\partial \rho}{\partial z} \right)^{1/2}$$

(where ρ is the fluid density, g is the acceleration of gravity, and z is the vertical coordinate), provides a measure of the stratification in units of s^{-1}, while shear is quantified by

$$S = \left(\frac{\partial u}{\partial z}^2 + \frac{\partial v}{\partial z}^2 \right)^{1/2}$$

(where u and v are components of horizontal velocity), also has units of s^{-1}.

The stratification during the dye release was relatively uniform in time, resulting principally from the strong vertical temperature gradient at the site (Fig. 2). The shear, on the other hand, was dominated by the internal tidal fluctuations, with the mean shear contributing less than 20% of the total. The vertical structure of the shear and stratification are shown in Fig. 16. The maximum shear occurred close to the target level of the dye, while the maximum stratification occurred slightly higher in the water column.

The gradient Richardson number

$$Ri = N^2/S^2$$

indicates the stability of the flow with respect to shear-induced mixing. For $Ri < 0.25$, the flow is unstable, and mixing will occur. Based on the rms shear and stratification (Fig. 16), the flow was stable for most of the water column, with $Ri > 1$ between 4 and 16-m depth. However, the fluctuations of shear and stratification caused fluctuations in Ri that produced frequent occurrences of $Ri < 0.25$. The distribution of Ri near the target level of the dye patch (8–12 m) for the five-day period is shown in Fig. 17. Roughly half of the estimates fall below 1, and 10% are less than 0.25. There was little variation from day to day in the proportion of $Ri < 0.25$. A similar fraction of $Ri < 0.25$ was observed during ADCP cruises in Massachusetts Bay in July–August 1990 as part of the Massachusetts Bays Program (Geyer, unpublished data). The magnitude of Ri depends on the

scale of the measurements; the proportion of $Ri < 0.25$ increases as the vertical scale becomes smaller. The resolution of the ADCP is 1-m, thus the estimates of Ri were limited to this scale.

4 Discussion

4.1 Mechanisms of Vertical Mixing

Internal tidal motions provided the dominant source of shear during this dye experiment, with non-tidal currents contributing less than 1/4th of the total shear. Because the wind-forced currents were unusually weak during the study, it is important to determine whether wind-driven shears could attain comparable magnitudes during other periods. Based on the observations during the Massachusetts Bays Program (Geyer et al., 1992), the wind-driven currents during summer months are generally smaller than the observed internal tidal fluctuations. The strongest wind-driven vertical shear observed during ADCP surveys in the summer of 1990 was approximately half the magnitude of the internal tidal shear. Although there may be occasional events in which wind-driven motions exceed the internal tidal shears, there is no evidence that wind-forced motions result in substantial vertical mixing events during the summer months, and in general it appears that internal tidal motions provide the driving energy for vertical mixing within the pycnocline.

The actual mechanisms of vertical mixing were not resolved in this study. That would require measurements at smaller vertical scales than could be accomplished with tow-yo sampling approach. Based on the existing theory and observations of stratified mixing processes (Gregg, 1989), it is likely that the mixing was due to shear instabilities resulting from a combination of internal tidal shears and small-scale internal waves. The internal tidal shears by themselves yield a value of $Ri \approx 1$, but temporal and/or spatial variations associated with propagating internal waves and bathymetric variations produced localized occurrences of $Ri < 0.25$, leading to vertical mixing. The significant incidence of $Ri < 0.25$ at 1-m vertical scale is consistent with the observation of active vertical mixing. Whether the rate of vertical mixing is consistent with the Richardson number statistics is a more difficult question, requiring knowledge of the high wavenumber variations of the shear and of the growth and evolution of instabilities. This is an area of current research.

4.2 Comparison with an Integrated Mixing Rate

The vertical mixing rate obtained in this dye release experiment was 0.04–0.08 $cm^2\ s^{-1}$. Based on analysis of the seasonal variations of temperature and salinity in the deep waters of Massachusetts Bay, Geyer et al., 1992 estimated an effective vertical mixing rate of 0.11–0.14 $cm^2\ s^{-1}$ for cross-isopycnal mixing during summer months. This difference between the local and global rates of vertical diffusion indicates either a) that the dye study occurred during a quiescent period relative to the seasonal average; b) that vertical mixing is more intense in other portions of the bay; or c) that processes other than vertical mixing, i.e., advection, contributed to the seasonal variation in temperature and salinity.

Based on the above discussion of the sources of vertical shear, it appears that the magnitude of the shears, and hence the mixing rate, was typical of this season. Although it is possible that large amounts of vertical mixing occur during rare events, the lack of strong winds and the persistence of strong stratification through the summer months argues against episodic mixing events.

The second possibility, that more intense mixing occurs elsewhere in the bay, is a reasonable explanation for the observed discrepancy. Although the irregular and sloping bathymetry in the vicinity of the dye patch would be conducive to strong internal tides and waves, the mixing would be expected to be more intense where the isopycnals intersect the bottom. There is still considerable controversy about how boundary mixing works and what contribution it makes to the total, but it remains an important candidate to explain the additional mixing required by the seasonal balance.

The third explanation, that advective processes other than mixing convey heat into and salt out of the deep water of the bay, remains a viable option. The analysis in Geyer et al., (1992) suggests that advective exchange does not occur between Massachusetts Bay and the adjoining Gulf of Maine. However, there could be advective motions associated with upwelling and downwelling that could contribute to vertical exchange. This process is related to the boundary mixing process; it could be that coupled mixing and advection in the boundary region contributes to enhanced cross-isopycnal exchange.

4.3 Mechanisms of Horizontal Mixing

The dye study provides an interesting example of oscillatory and mean shear dispersion (Fischer et al., 1979). During the first several days of spreading, the oscillatory shears of the internal tide dominated the dispersion, and the dye spread out nearly

isotropically due to the variable direction of the internal tidal motions. After the third day, the less energetic but more persistent mean shears began to influence the growth of the patch, and it became elongated in the direction of the mean flow. The increase in the horizontal dispersion rate between days 3 and 4 is likely related to an increase in the mean shear in the N–S direction. The ADCP data do indicate an increase in N–S shear between days 3 and 4, with northward-directed flow above the level of the dye and southward-directed flow beneath. This mean flow should result in a tilting of the patch, with the northern portion of the patch higher in the water column than the southern portion. This tendency is indicated in the N–S dye section from day 5 (Fig. 18).

Okubo's (1971) empirical estimates of oceanic mixing indicate a value of $K \approx 3$ m^2 s^{-1} for the 4–6 km patch size of the dye experiment. The observed spreading rates for the first several days are consistent with Okubo, but the more rapid spreading on days 4 and 5 (see Table 1) is significantly greater. Okubo's results are based on horizontal mixing in the surface mixed layer, while the present experiment was conducted in the thermocline. The much weaker vertical mixing in the thermocline than the mixed layer should lead to larger horizontal dispersion rate, based on shear dispersion theory (Fischer et al., 1979). This may explain the discrepancy. There is little other empirical information to draw from for comparison, but the problem should be amenable to more detailed theoretical analysis.

Acknowledgements

The authors wish to thank Terry Donahue, Stewart Sutherland and Craig Marquette for their assistance during the field work. Fran Hotchkiss and Richard Signell of the U.S. Geological Survey kindly provided timeseries data. The chlorophyll fluorometer was graciously loaned to us by Battelle/Duxbury. This work was partially funded by the Massachusetts Water Resources Authority and SeaGrant grant R10-17. Its conclusions reflect the opinions of the authors and not necessarily those of the MWRA.

5 References

Blumberg, A. F., R. P. Signell and H. L. Jenter, 1993. Modelling transport processes in the coastal ocean. *J. Mar. Env. Eng.*, **1**, 31–52.

Fischer, H. B., E. J. List, R. C. Y. Kho, J. Imberger and N.H. Brooks, 1979. *Mixing in Inland and Coastal Waters*, Academic Press, New York. 483 pp.

Geyer, W. R., G. B. Gardner, W. S. Brown, J. Irish, B. Butman, T. Loder, and R. Signell, 1992. Physical oceanographic investigation of Massachusetts and Cape Cod Bays, MBP-92-03, Massachusetts Bays Program, 497 pp.

Gregg, M. C., 1987. Diapycnal mixing in the thermocline: A review. *J. Geophys. Res.*, **92**, 5249–5286.

Lin, J. T. and Y. H. Pao, 1979. Wakes in stratified fluids. *Ann. Rev. Fluid Mech.*, **11**, 317-338.

Okubo, A, 1971. Oceanic diffusion diagrams. *Deep-Sea Res.*, **18**, 789–802.

Townsend, D. W., L. M. Cammen, J. P. Christensen, S. G. Ackleson, M. D. Keller, E. M. Hougen, S. Corwin, W. K. Bellows and J. F. Brown, 1990. Oceanographic conditions in Massachusetts Bay in early and late summer: Cruise results from 5 June and 14 August, 1990. Bigelow Laboratory for Ocean Sciences Technical Report No. 80.

Table 1: Horizontal Dispersion of Dye Patch

σ_{E-W} and σ_{N-S} are moments of the patch in the E-W and N-S directions, respectively. σ is the rms moment. σ_c is the moment, corrected for the integrated mass of the patch. K and K_c are the horizontal dispersion coefficients based on σ and σ_c.

Day No.	σ_{E-W} (m)	σ_{N-S} (m)	σ (m)	σ_c (m)	K $(m^2 s^{-1})$	K_c $(m^2 s^{-1})$
1	~500	~500	500	500		
					3.1	1.9
2	1100	1200	1151	946		
					2.9	4.2
3	1200	1800	1530	1530		
					5.7	18.6
4	1700	2400	2080	2960		
					16.4	14.8
5	2000	4000+	3160	3727		

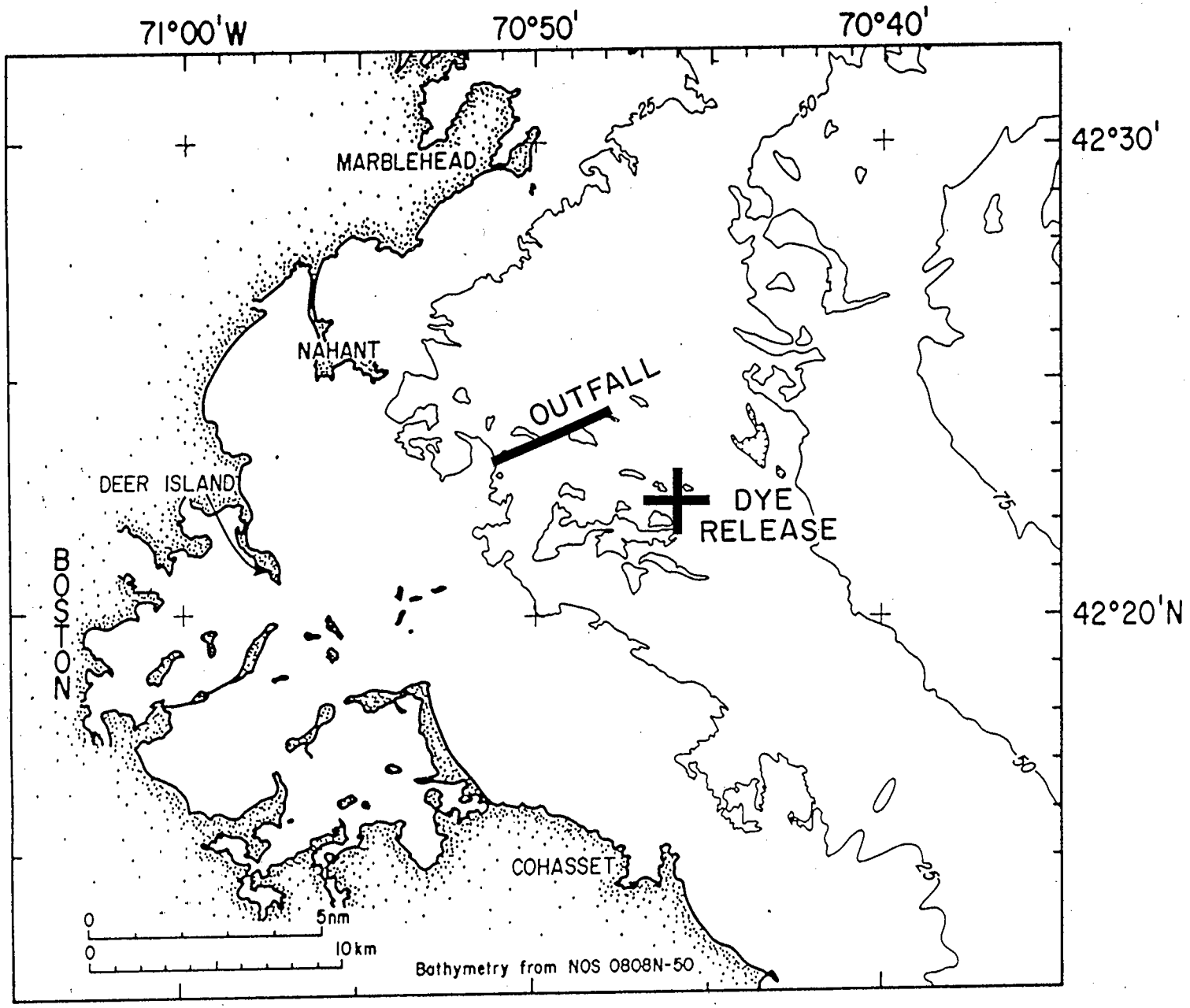

1. Western Massachusetts Bay, showing the location of the dye release and the new sewage outfall. The water depth is approximately 30-m, with numerous bathymetric irregularities.

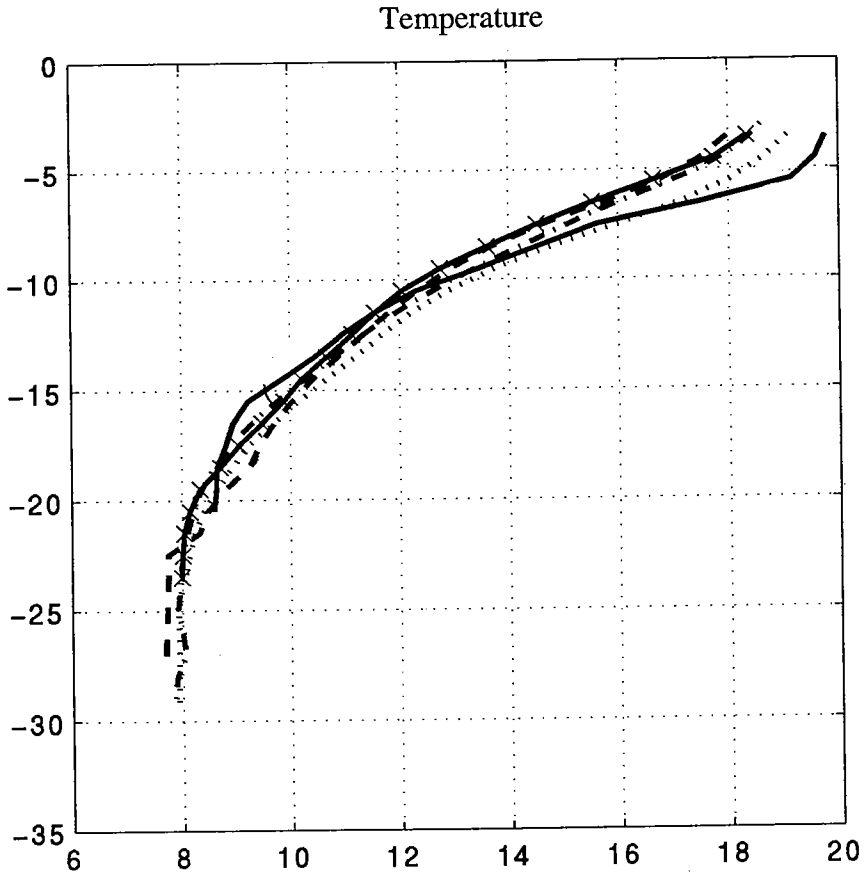

2. Daily average temperature profiles for the 5 days of the dye experiment. The temperature stratification makes a dominant contribution to the density gradient, although salt stratification also contributes. The target level of the dye was 12.5°, approximately 10-m deep in the middle of the thermocline.

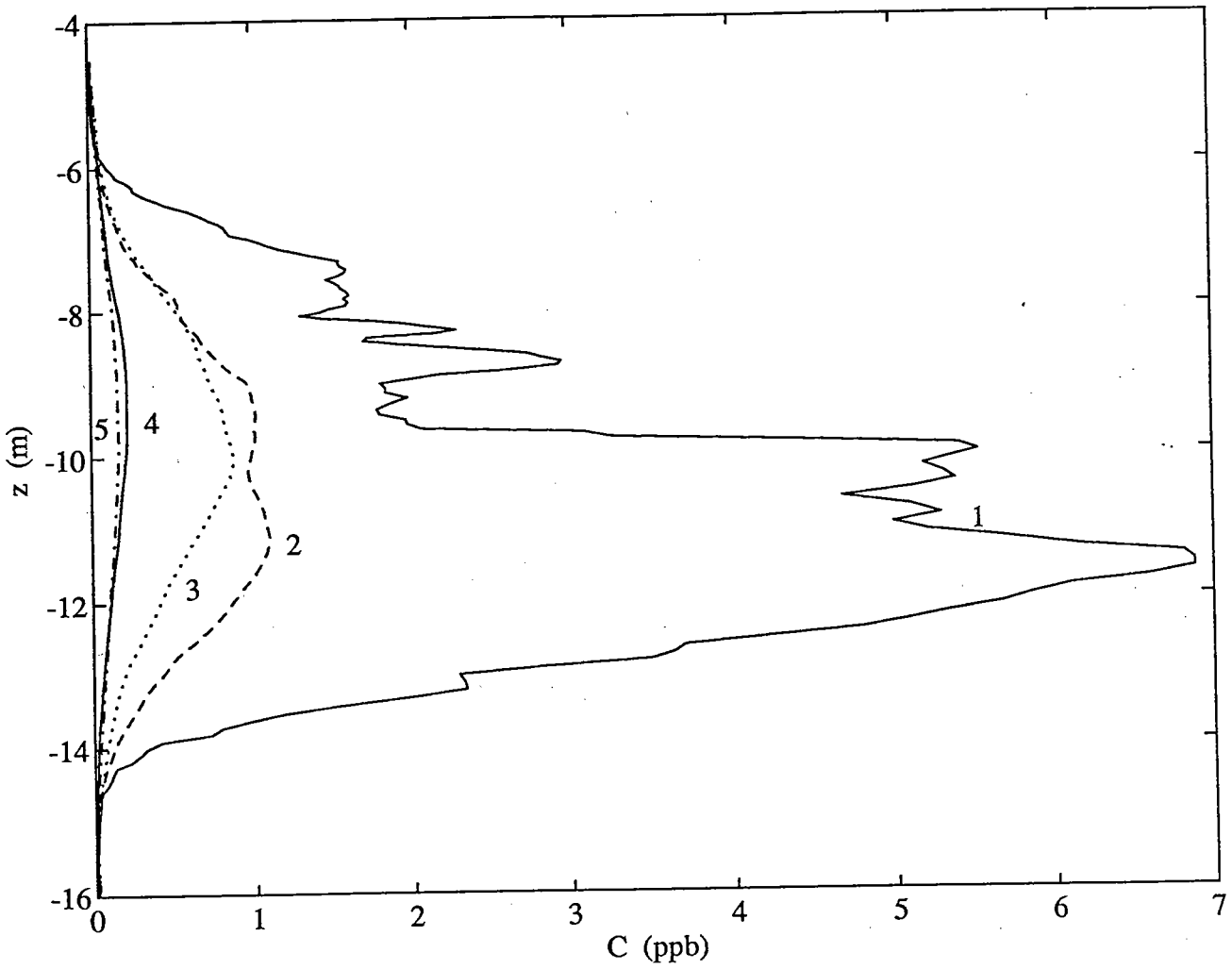

3. Daily average vertical dye distributions in parts per billion (ppb). The averaging was done as a function of temperature rather than depth, and the profiles were remapped onto a depth coordinate based on the average temperature profile. This use of isopycnal coordinates removes the large distortions associated with internal waves and low-frequency isopycnal displacements. The irregularity of the concentration profile in day 1 is due to a small number of profiles within the dye patch. Likewise there were inadequate profiles during day 2 to obtain high quality statistics of the dye distribution.

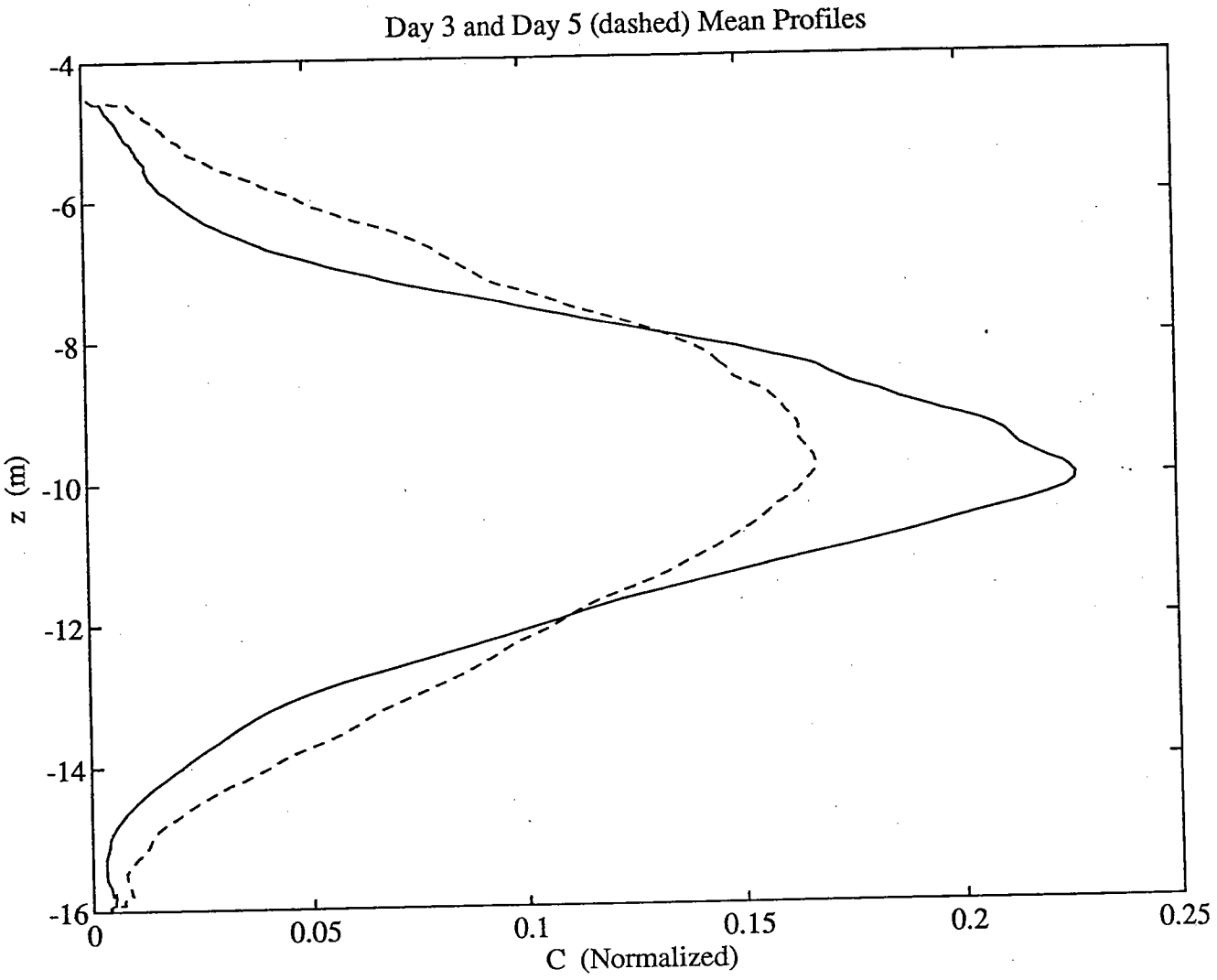

4. Daily average dye distributions from days 3 and 5, normalized to the same area. Again isopycnal coordinates were used for the averaging. The vertical spreading of the dye is evident in the broadening of the shoulders of the distribution between days 3 and 5.

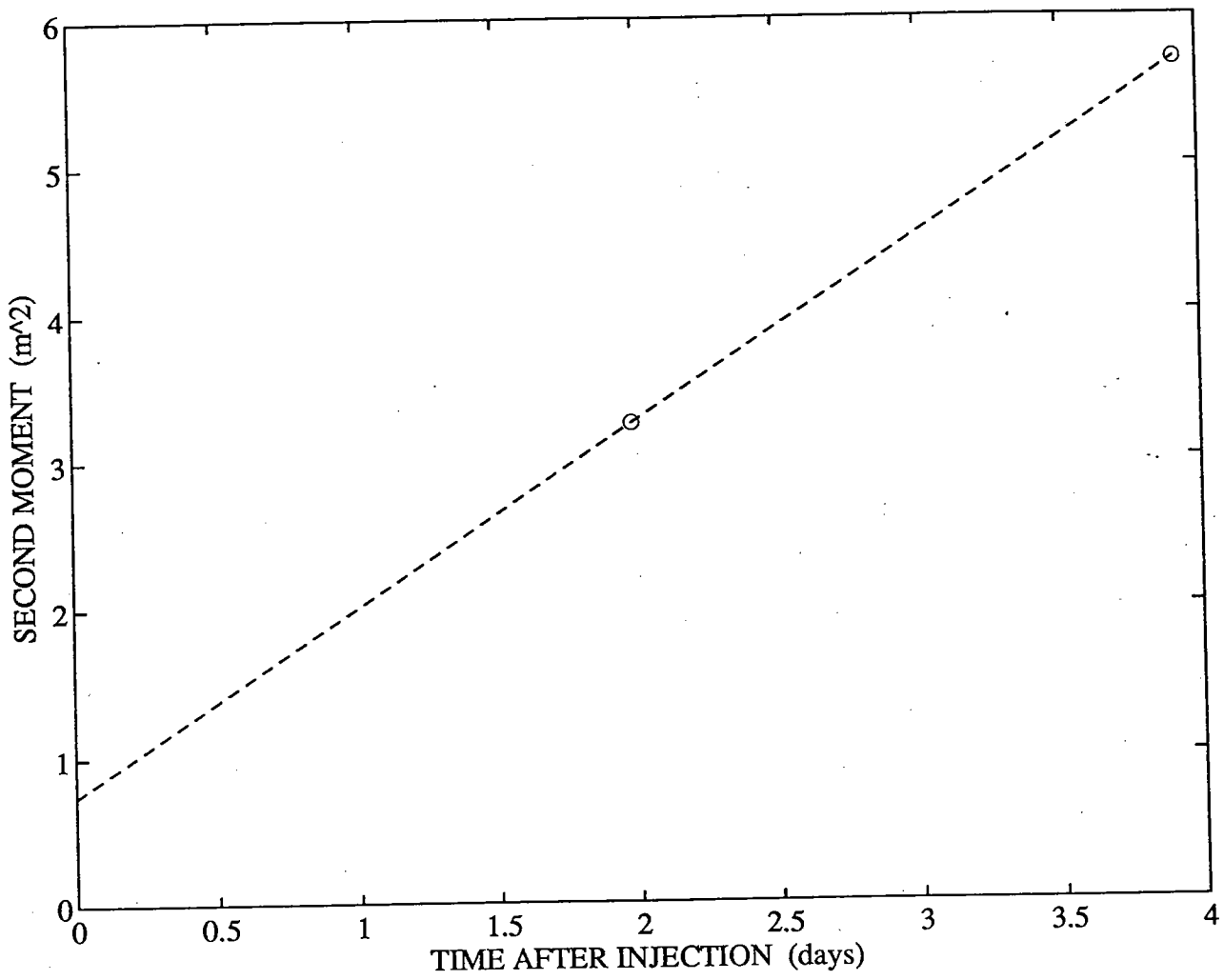

5. Temporal evolution of the second moment σ^2 between days 3 and 5. The vertical diffusivity is estimated based on this spreading rate to be $K_z = 0.04 - 0.08$ cm^2 s^{-1}.

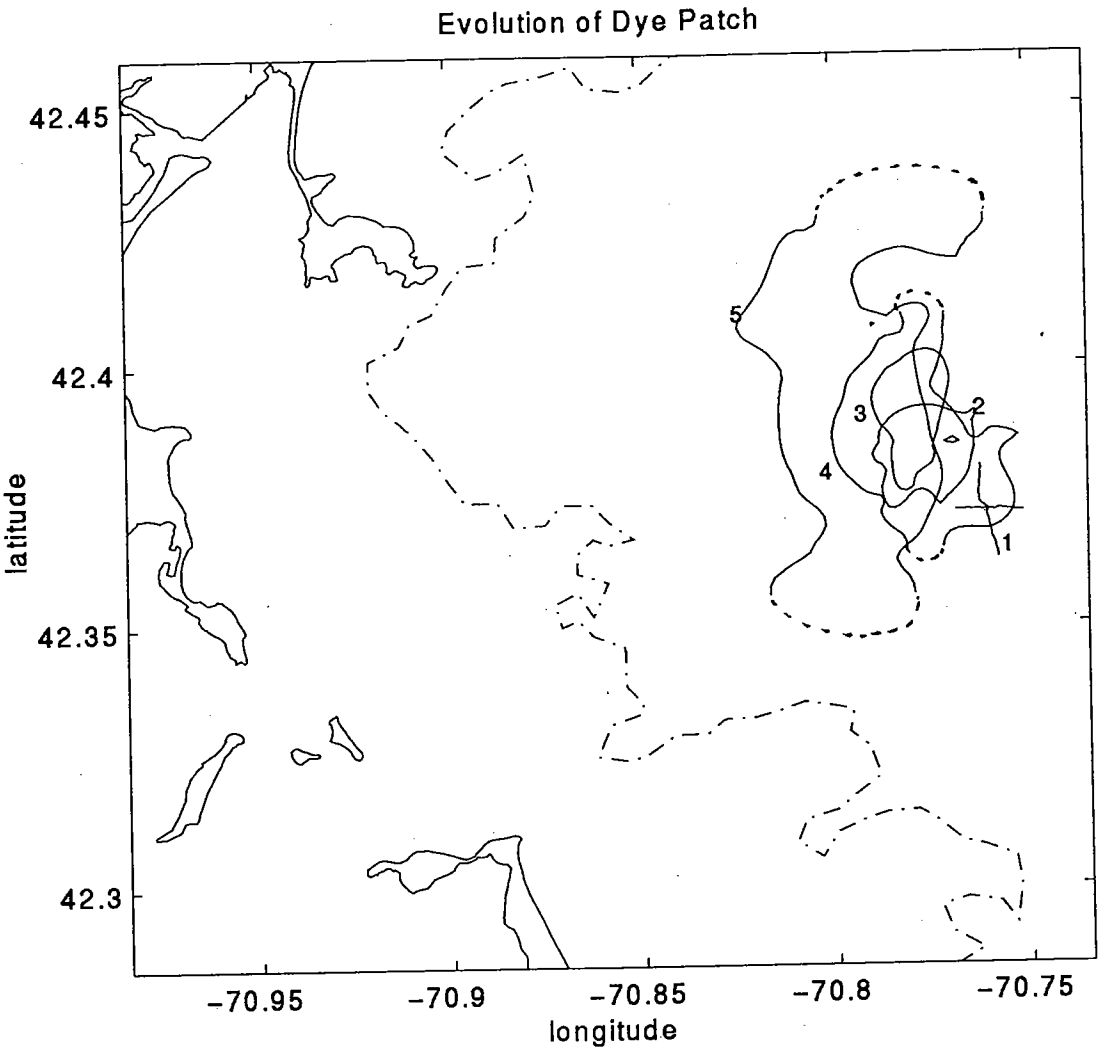

6. Evolution of the horizontal distribution of dye, from its release as a "+" on day 1 to its growth into an elongated blob on day 5. The boundaries of the patch are defined by the contour at which the dye is roughly one third of its maximum value. See Fig. 7 for detailed maps of the dye distribution.

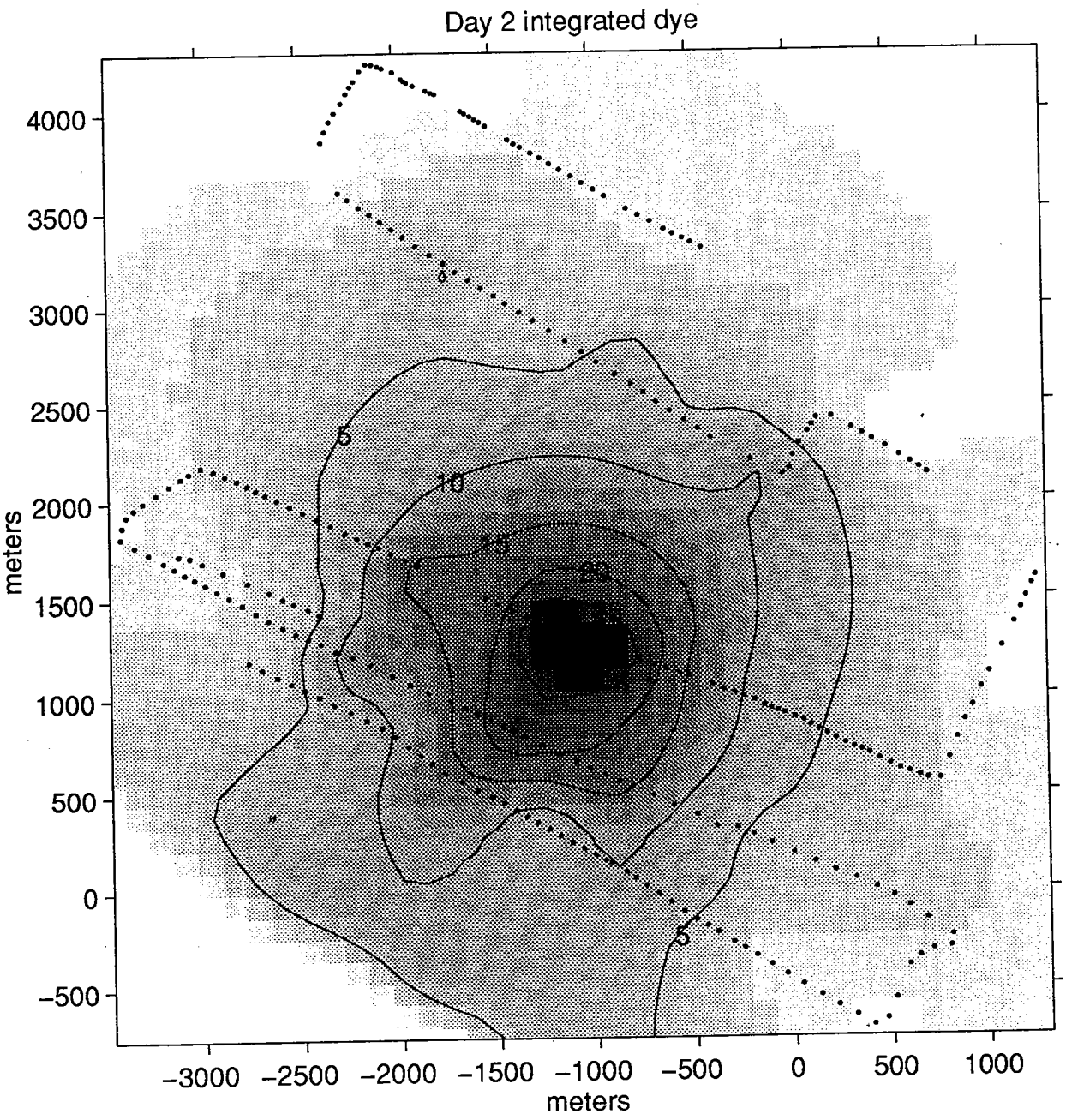

7. Contours of the vertically integrated dye distributions for days 2, 3, 4 and 5. The units are kg km^{-}2. The individual profiles are indicated by dots. In order to remove the excessive distortion of the apparent distribution due to tidal advection through the course of the survey, the plots are constructed in a Lagrangian reference frame, with the positions of each sampling point translated based on the observed velocity at the target level of the dye. Note that the data are extrapolated beyond the region bounded by the observations.

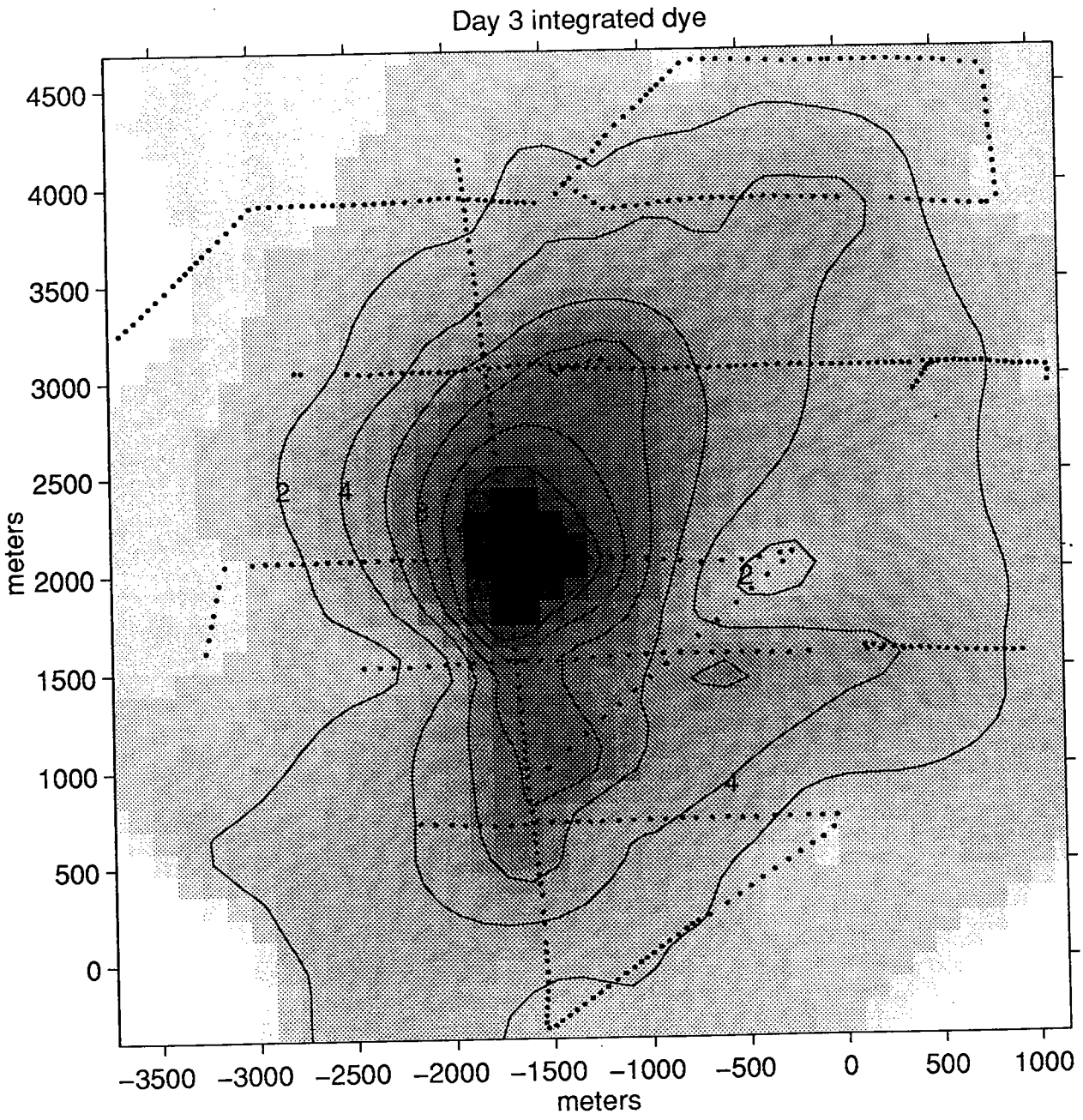
Day 3 integrated dye
meters
4500
4000
3500
3000
2500
2000
1500
1000
500
0
2
4
2
4
−3500
−3000
−2500
−2000
−1500
−1000
−500
0
500
1000
meters

7. (Continued)

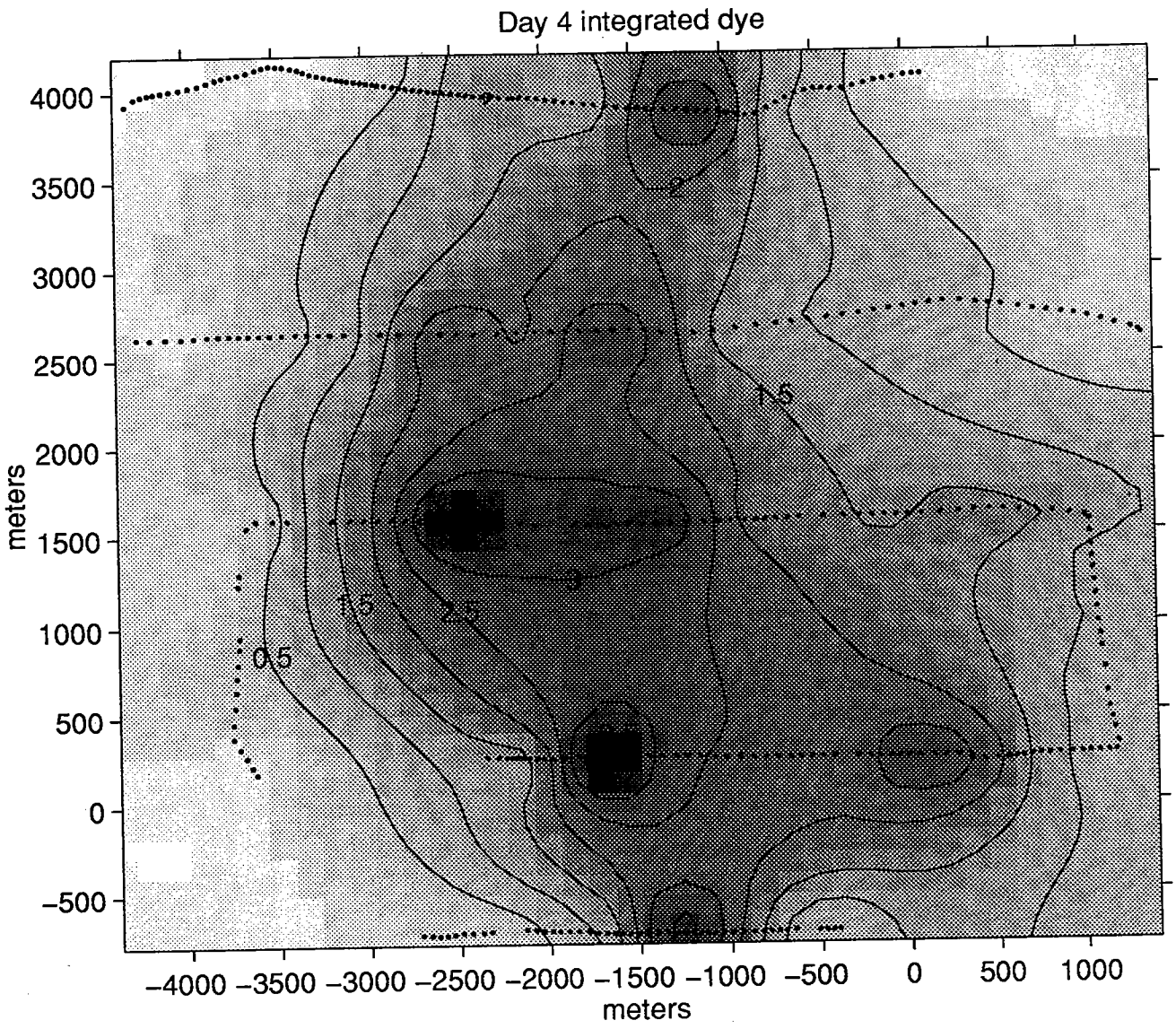
Day 4 integrated dye
4000
3500
3000
2500
2000
1500
1000
500
0
−500
meters
0.5
1.5
2.5
3
1.5
−4000 −3500 −3000 −2500 −2000 −1500 −1000 −500 0 500 1000
meters

7. (Continued)

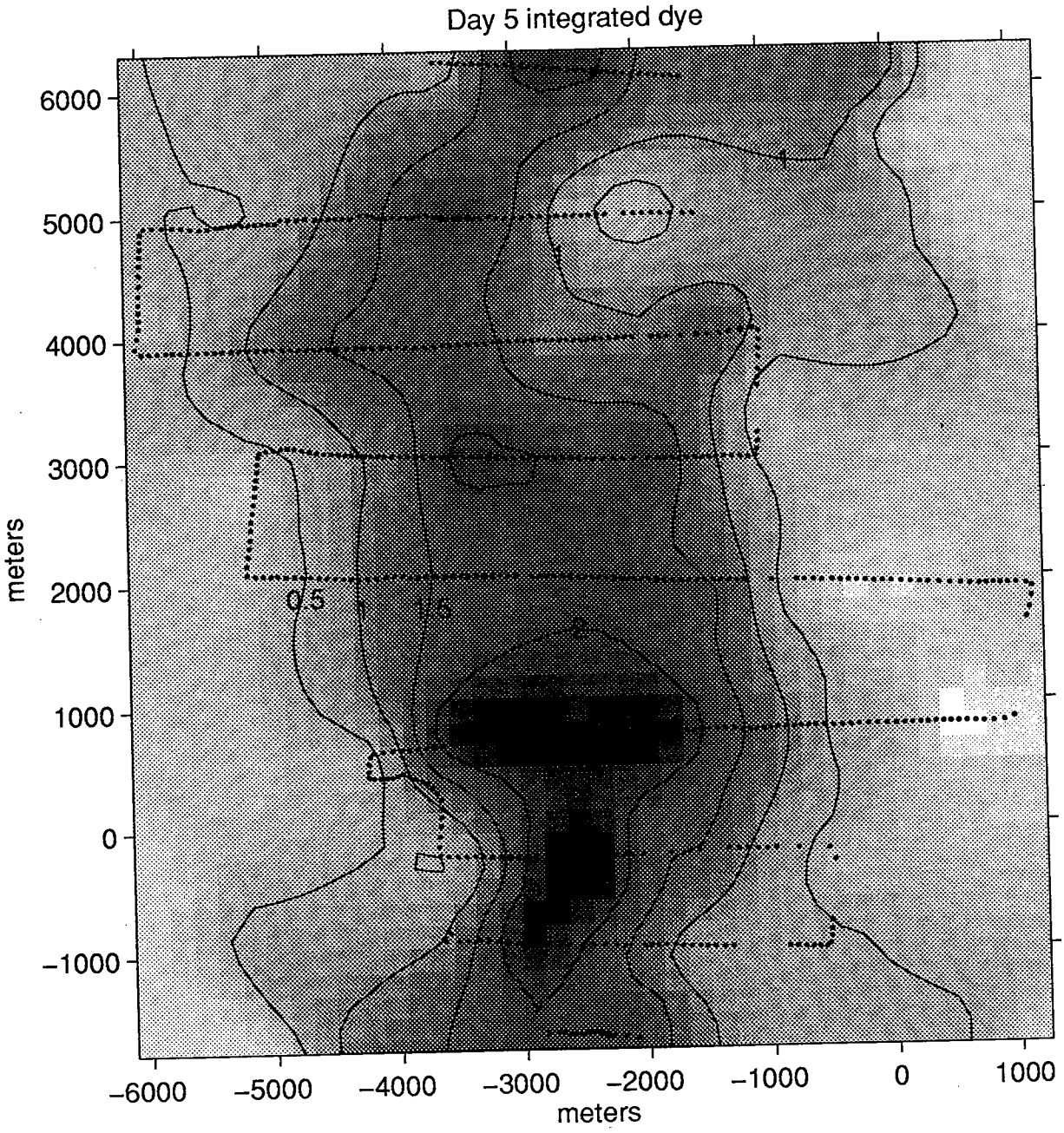
Day 5 integrated dye
6000
5000
4000
3000
2000
1000
0
−1000
meters
0.5
1
1.5
2
−6000
−5000
−4000
−3000
−2000
−1000
0
1000
meters

7. (Continued)

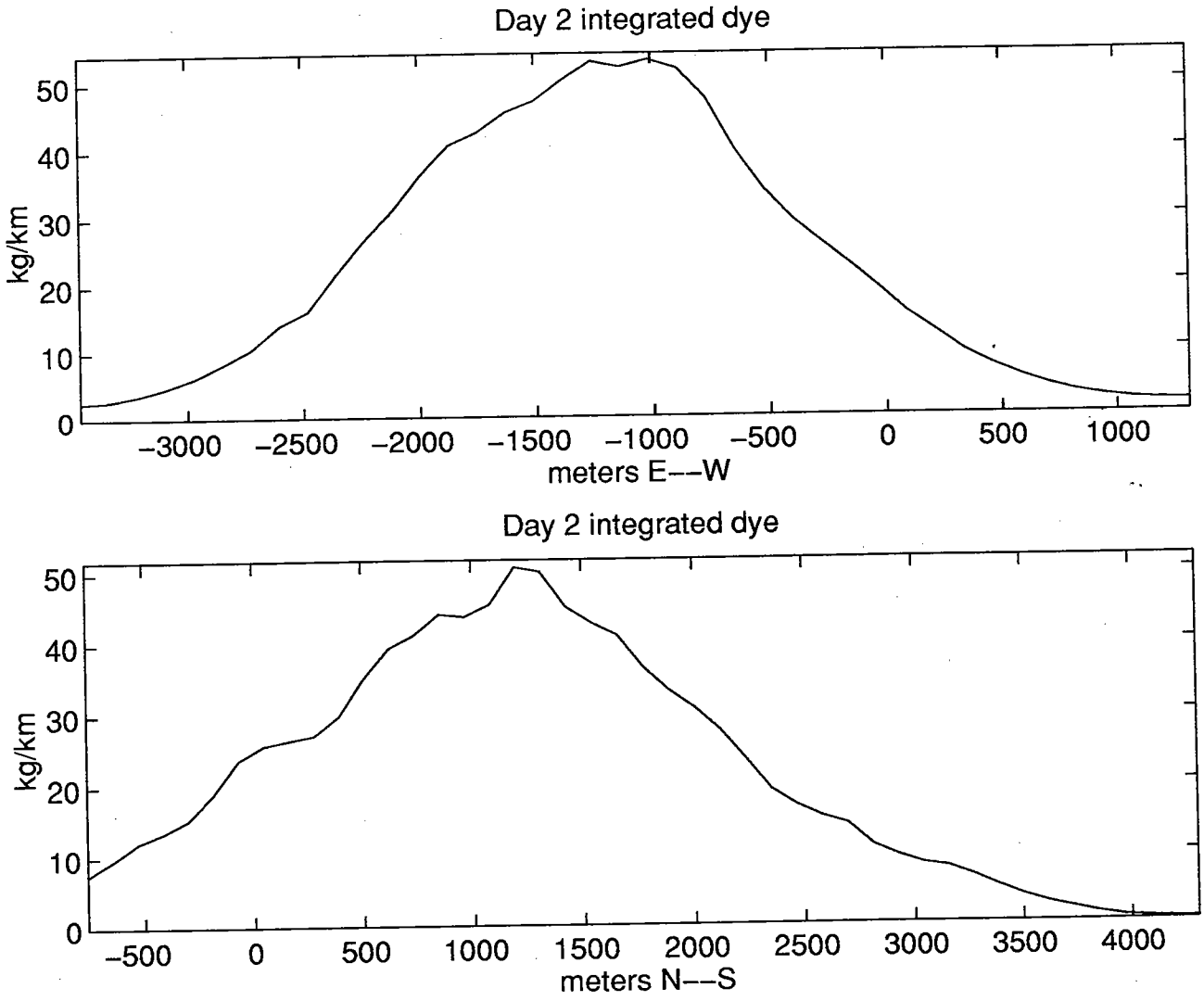

8. E–W and N–S sections of the vertically and horizontally integrated dye distributions for days 2, 3, 4 and 5. The initial spreading of the dye is isotropic and the distributions are nearly Gaussian, but subsequent evolution of the patch shows more rapid growth in the N–S direction. The horizontal dispersion rates based on these distributions are shown in Table 1.

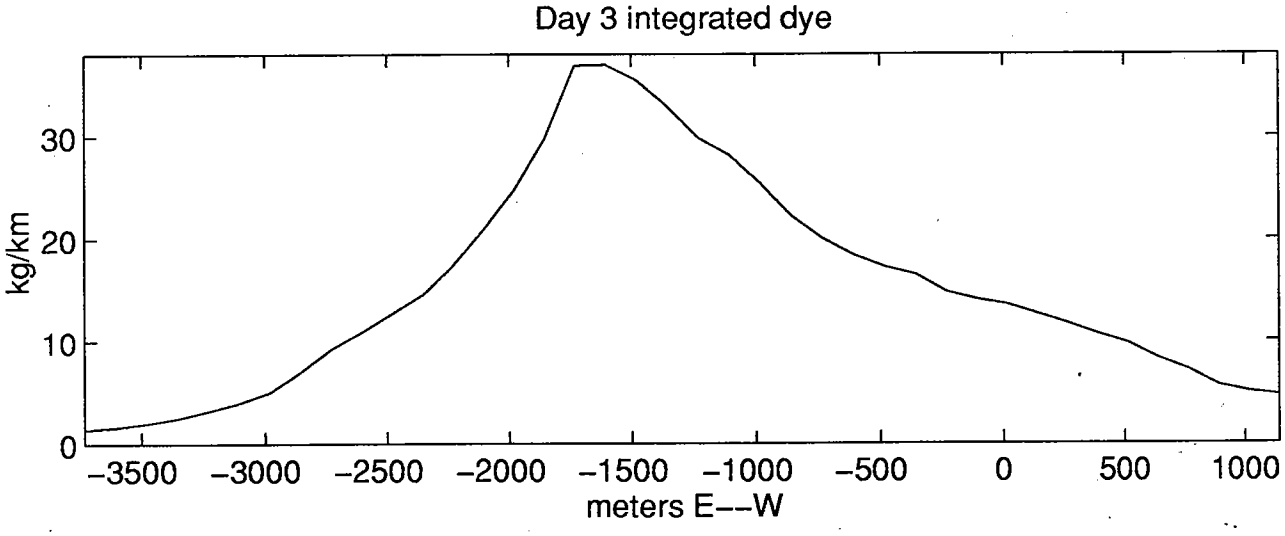
Day 3 integrated dye
kg/km
30
20
10
0
−3500 −3000 −2500 −2000 −1500 −1000 −500 0 500 1000
meters E−−W

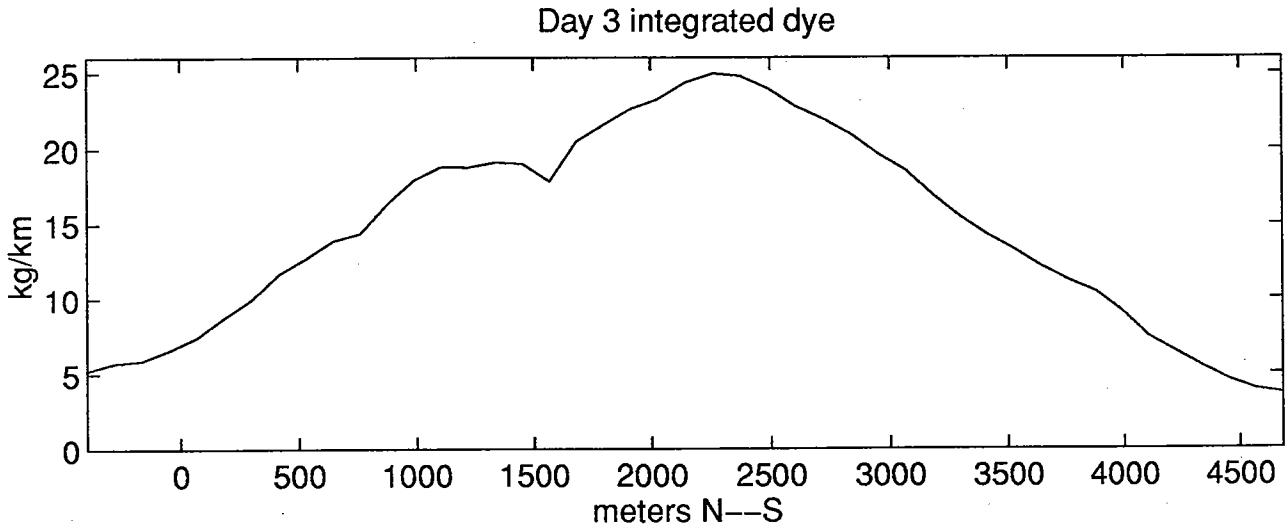
Day 3 integrated dye
kg/km
25
20
15
10
5
0
0 500 1000 1500 2000 2500 3000 3500 4000 4500
meters N−−S

8. (Continued)

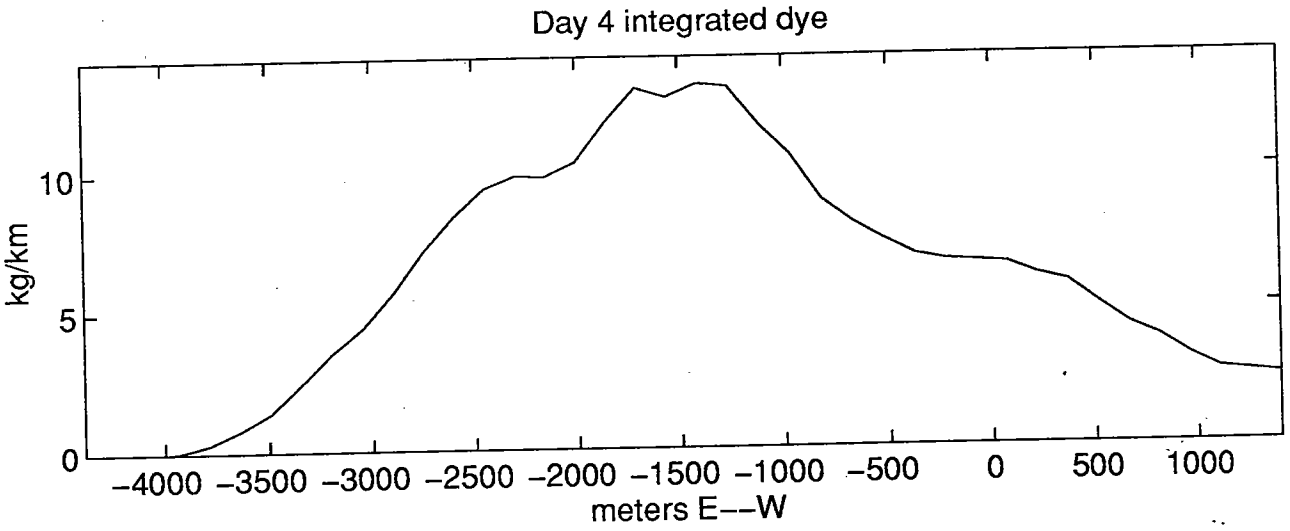
Day 4 integrated dye
kg/km
10
5
0
−4000 −3500 −3000 −2500 −2000 −1500 −1000 −500 0 500 1000
meters E−−W

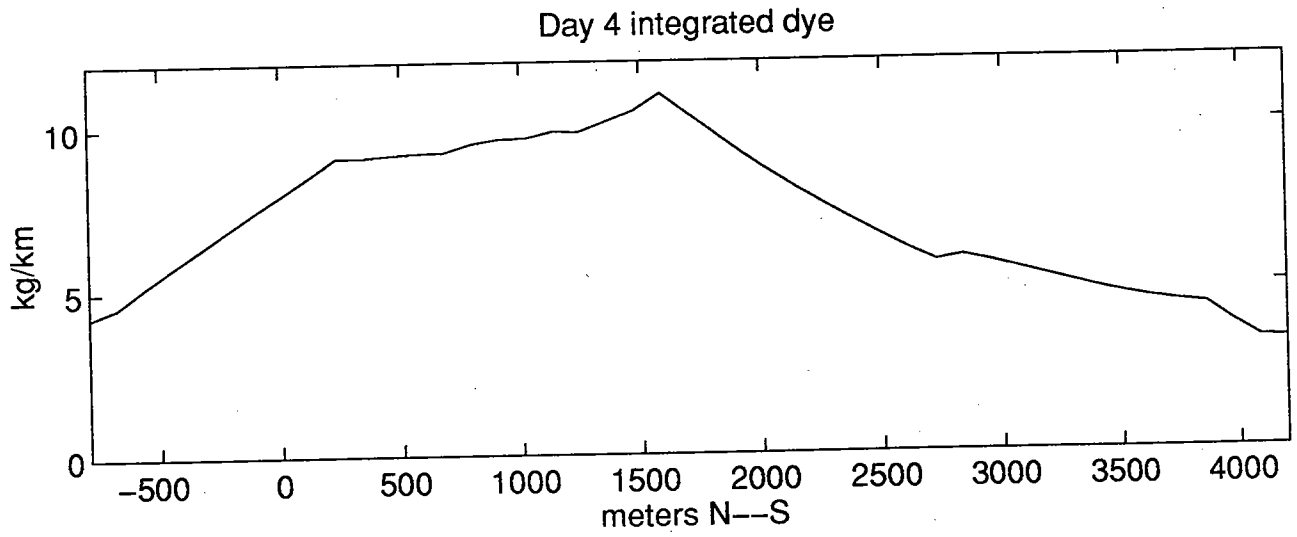
Day 4 integrated dye
kg/km
10
5
0
−500 0 500 1000 1500 2000 2500 3000 3500 4000
meters N−−S

8. (Continued)

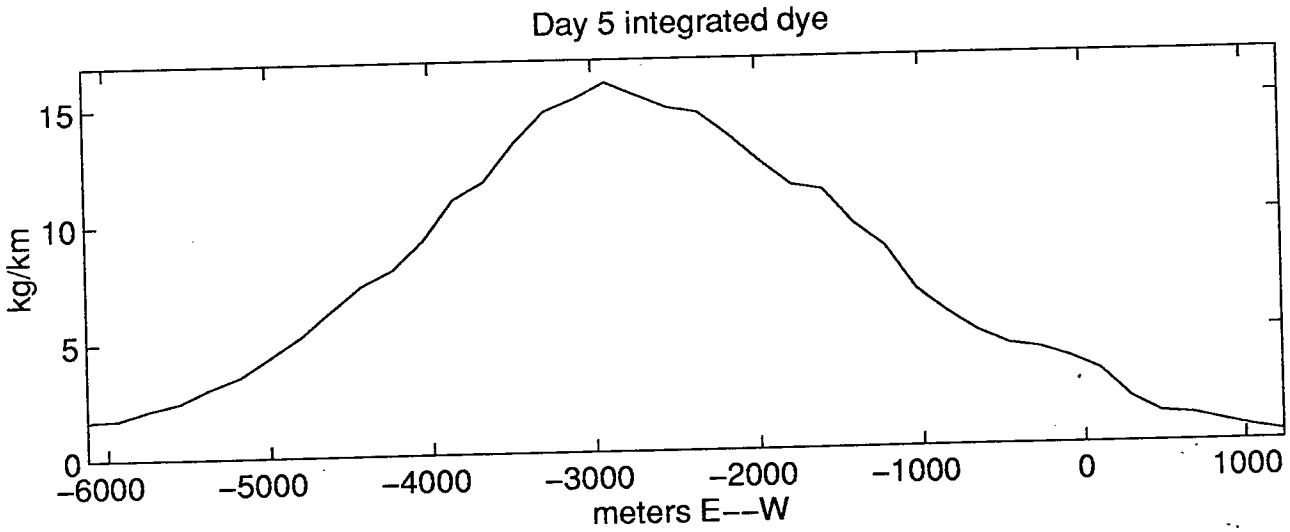
Day 5 integrated dye
15
10
5
0
kg/km
−6000
−5000
−4000
−3000
−2000
−1000
0
1000
meters E−−W

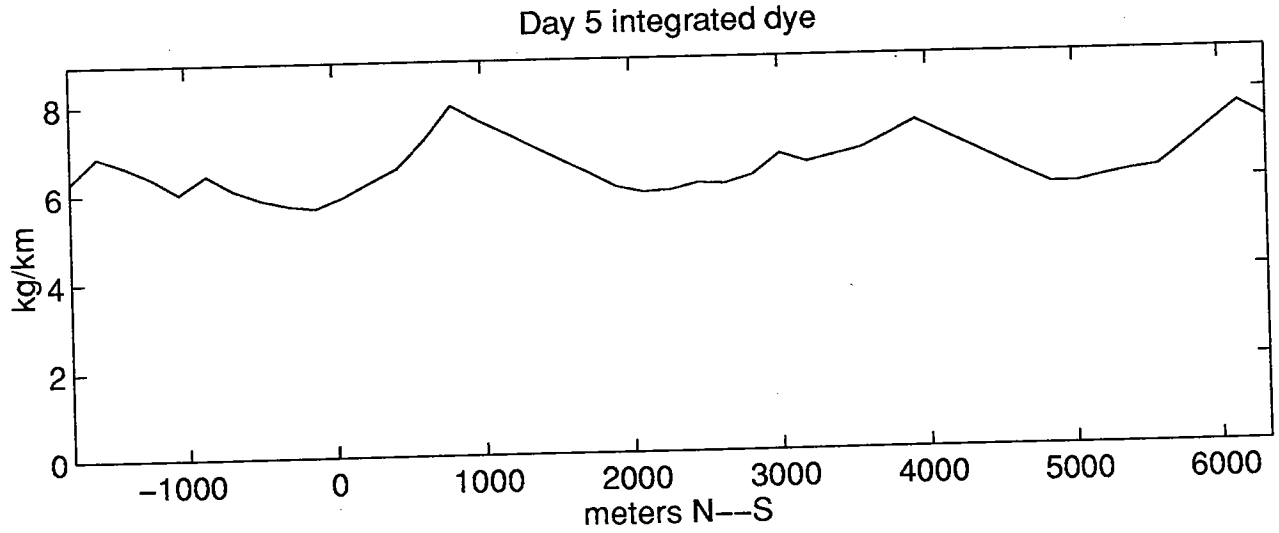
Day 5 integrated dye
8
6
4
2
0
kg/km
−1000
0
1000
2000
3000
4000
5000
6000
meters N−−S

8. (Continued)

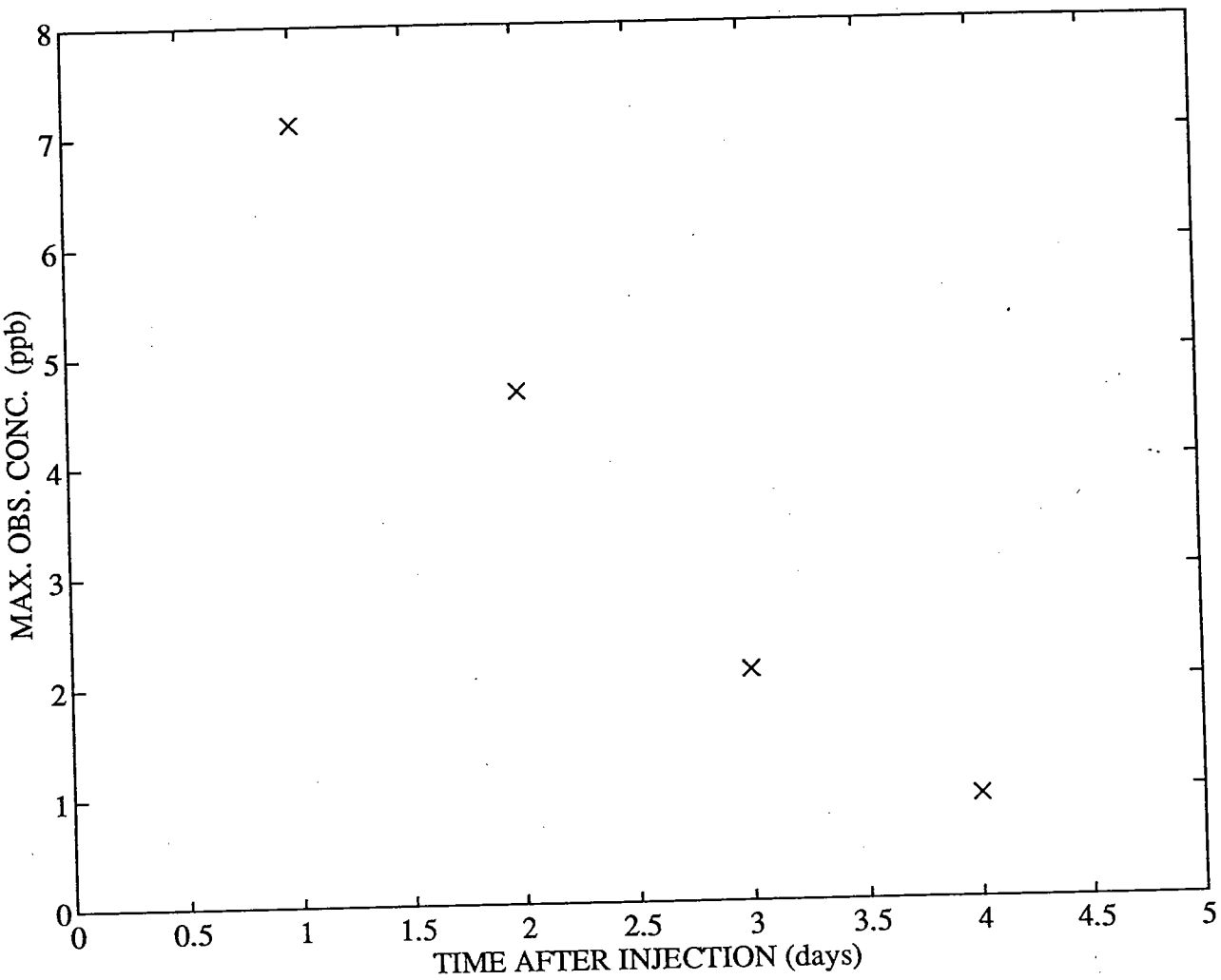

9. Temporal evolution of the maximum observed dye concentration within the patch. The sharp and consistent reduction in concentration with time indicates that mixing is occurring in conjunction with the spreading of the patch, i.e., there are not localized blobs of undiluted dye. This does not provide proof that there are not small patches of high concentration, but the mass balance estimates suggest that there is little dye that is not accounted for (in fact too much dye is accounted for!)

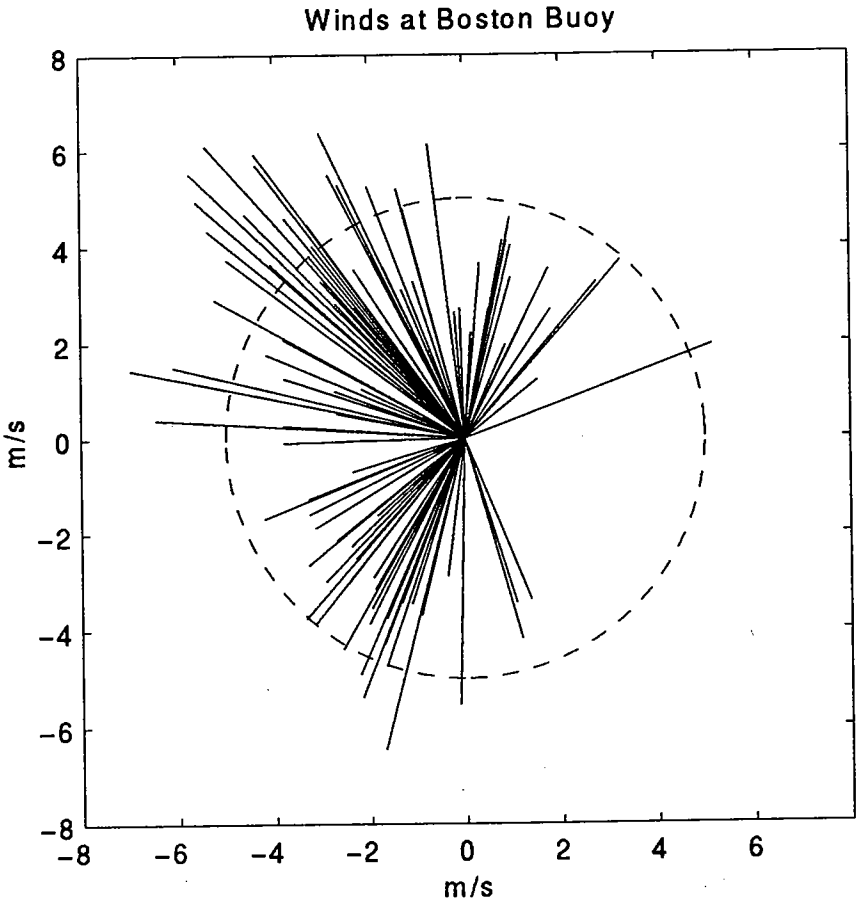

10. Wind vectors (a) (pointing in direction wind is blowing) and wind timeseries (b) obtained at the Boston meteorological buoy near the position of the dye release. The days of the dye survey are indicated on the timeseries. Winds were generally from the easterly quadrants during this period, which is unusual.

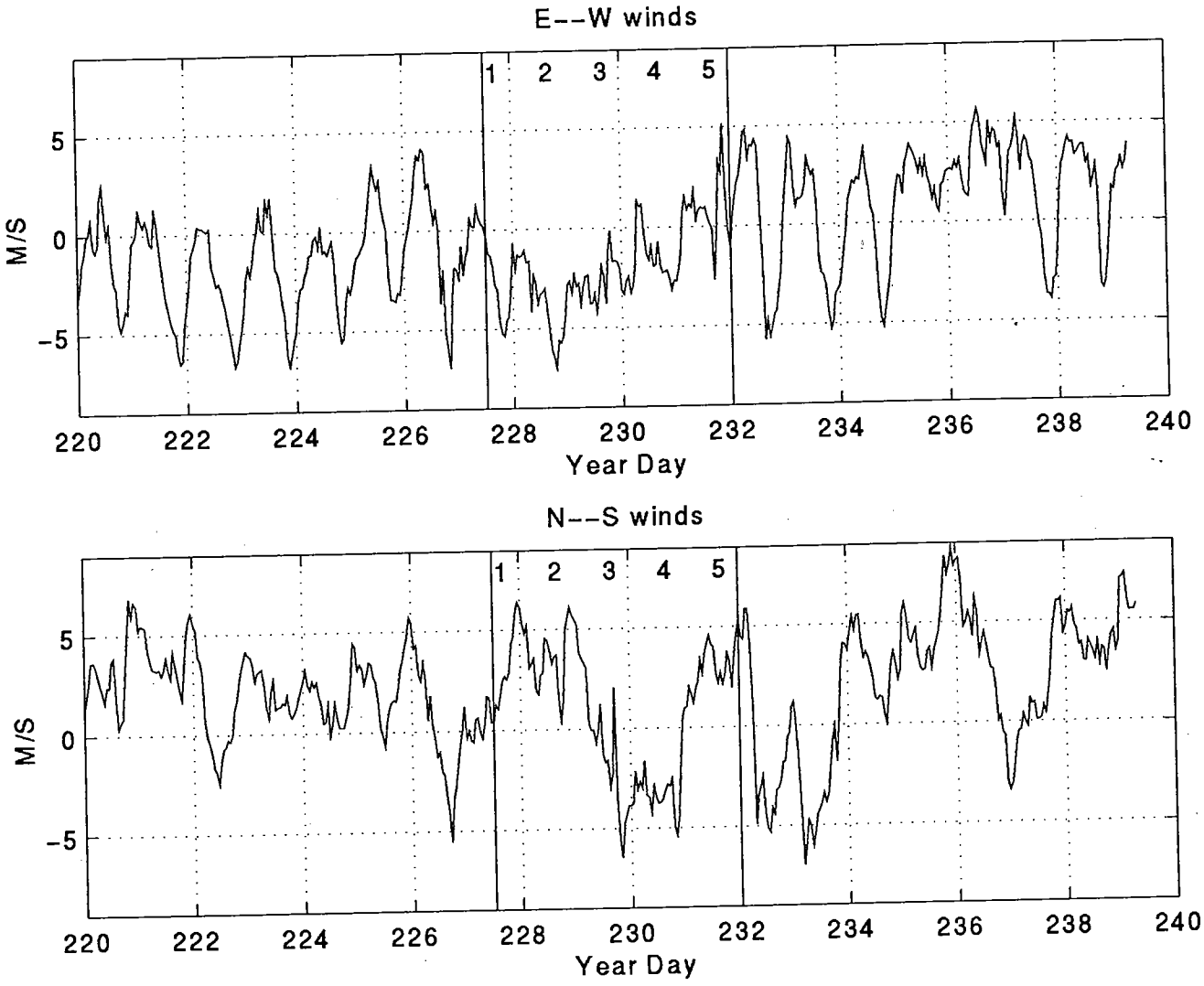

10. (Continued)

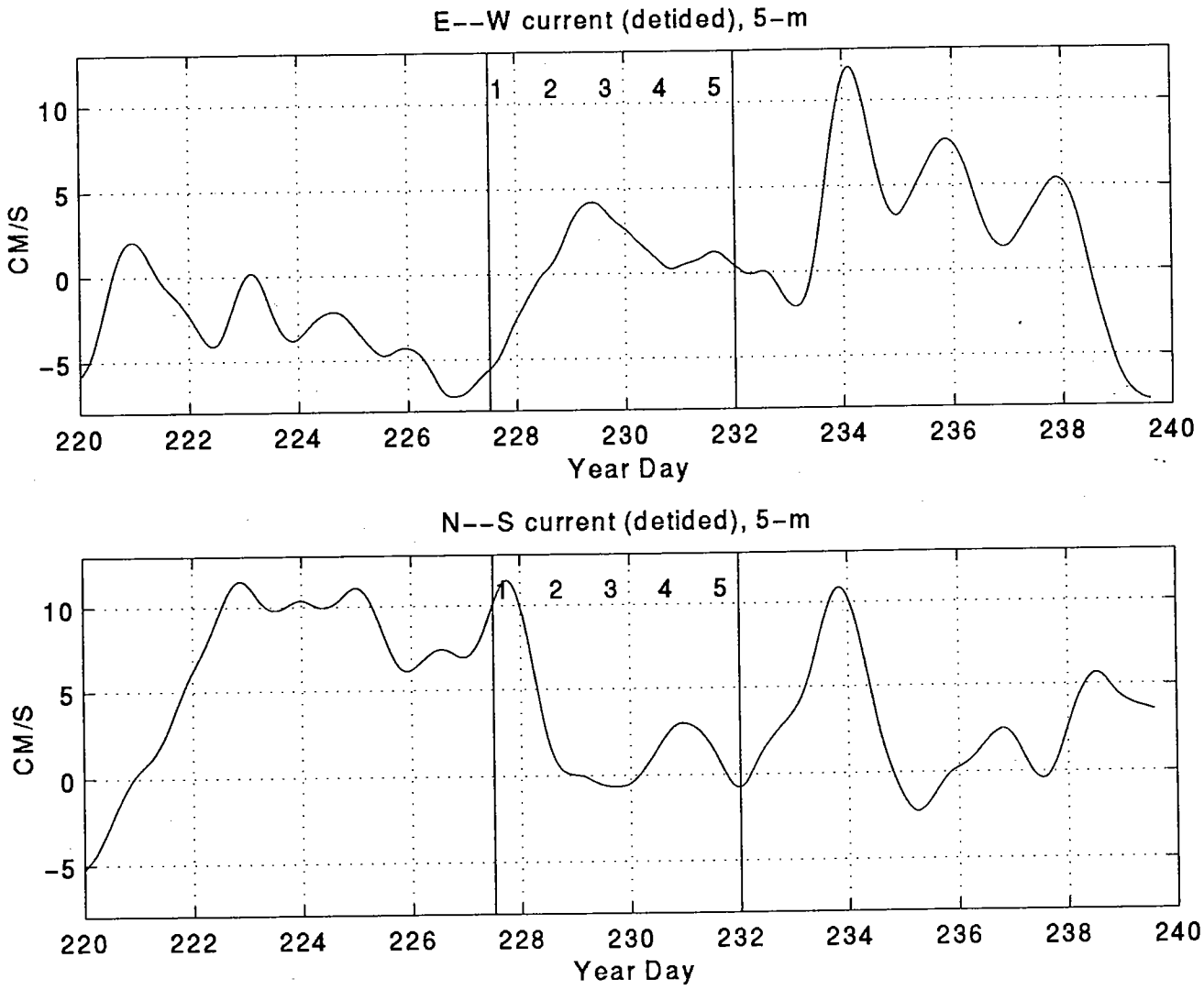

11. Tidally averaged (35-hour filtered) currents from the U.S. Geological Survey instrument at 5-m depth at the Boston meteorological buoy before, during and after the dye study. Except for day 1, the non-tidal currents were very weak during the study. These currents were 5-m above the dye, so they differ in detail from the currents advecting the dye patch, but they provide a qualitative view of the conditions.

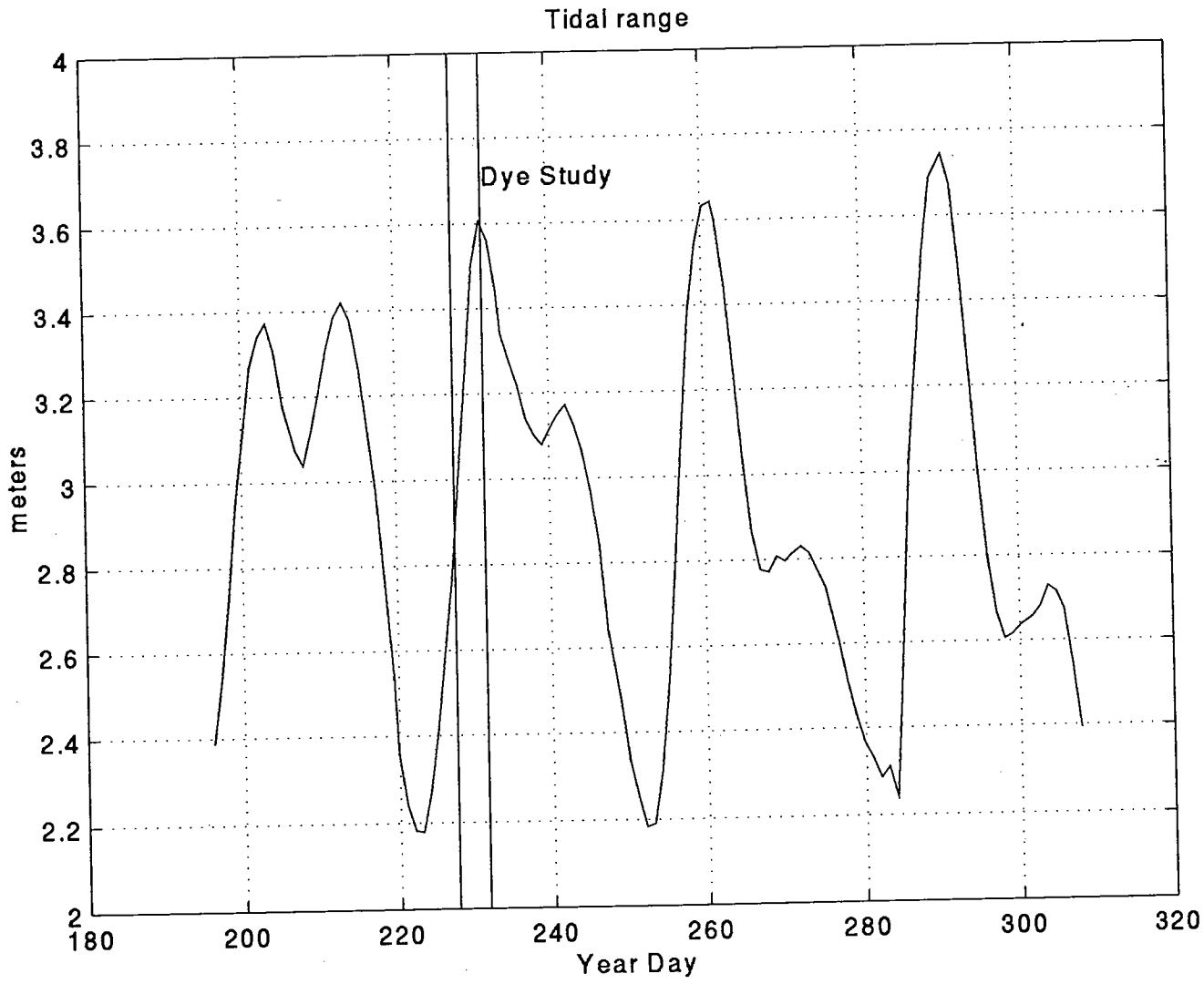

12. Tidal range before, during and after the dye study, based on U.S. Geological Survey pressure records at the bottom at the location of the Boston meteorological buoy. The dye study started at a point intermediate between neap and spring tides, and ended during spring tides.

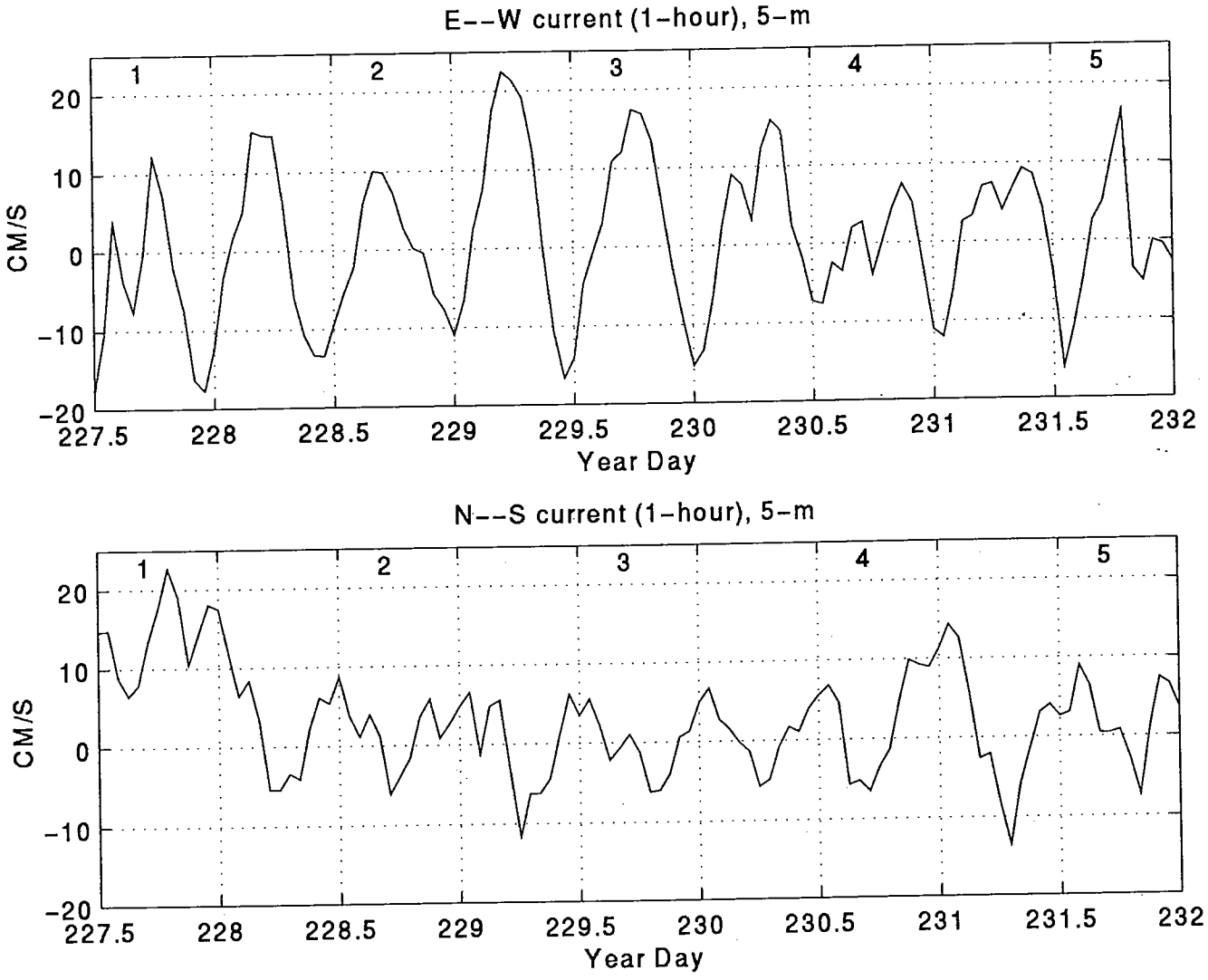

13. Hourly currents at 5-m depth at the Boston meteorological buoy, from the U.S. Geological Survey mooring. Although tidal amplitudes were increasing monotonically during the deployment period, the tidal velocities at 5-m depth showed a more irregular pattern. This was due to the important influence of internal tides, which can augment or reduce the barotropic component of tidal motion at a given level.

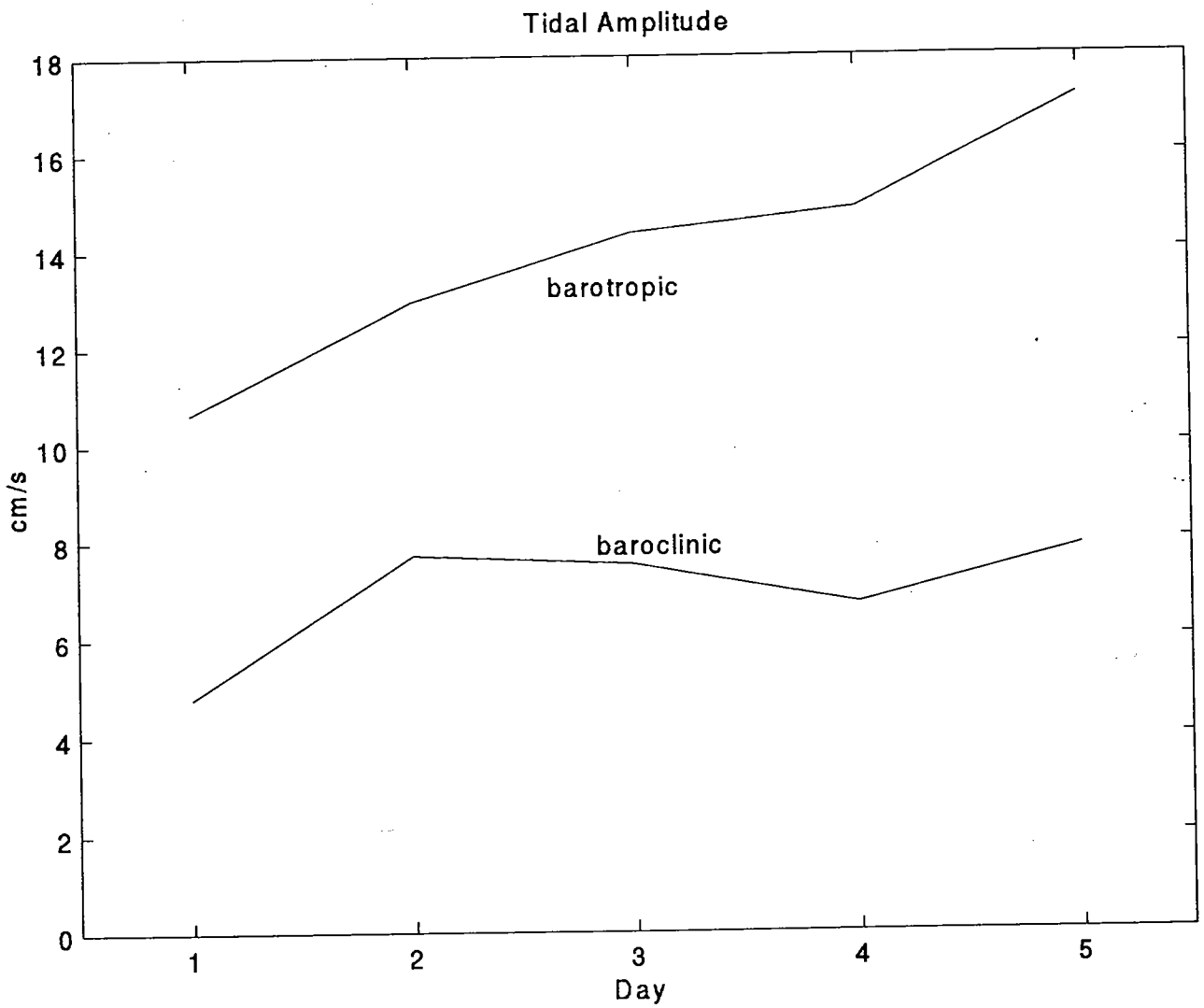

14. Variation of amplitude of the barotropic (vertically averaged) and baroclinic (vertically varying) semi-diurnal tidal currents, based on the ADCP measurements. The barotropic component shows the monotonic increase indicated by the pressure record, while the baroclinic component is more variable. The baroclinic component is approximately half of the barotropic – an unusually large fraction that is due to the strong stratification and steep bathymetry.

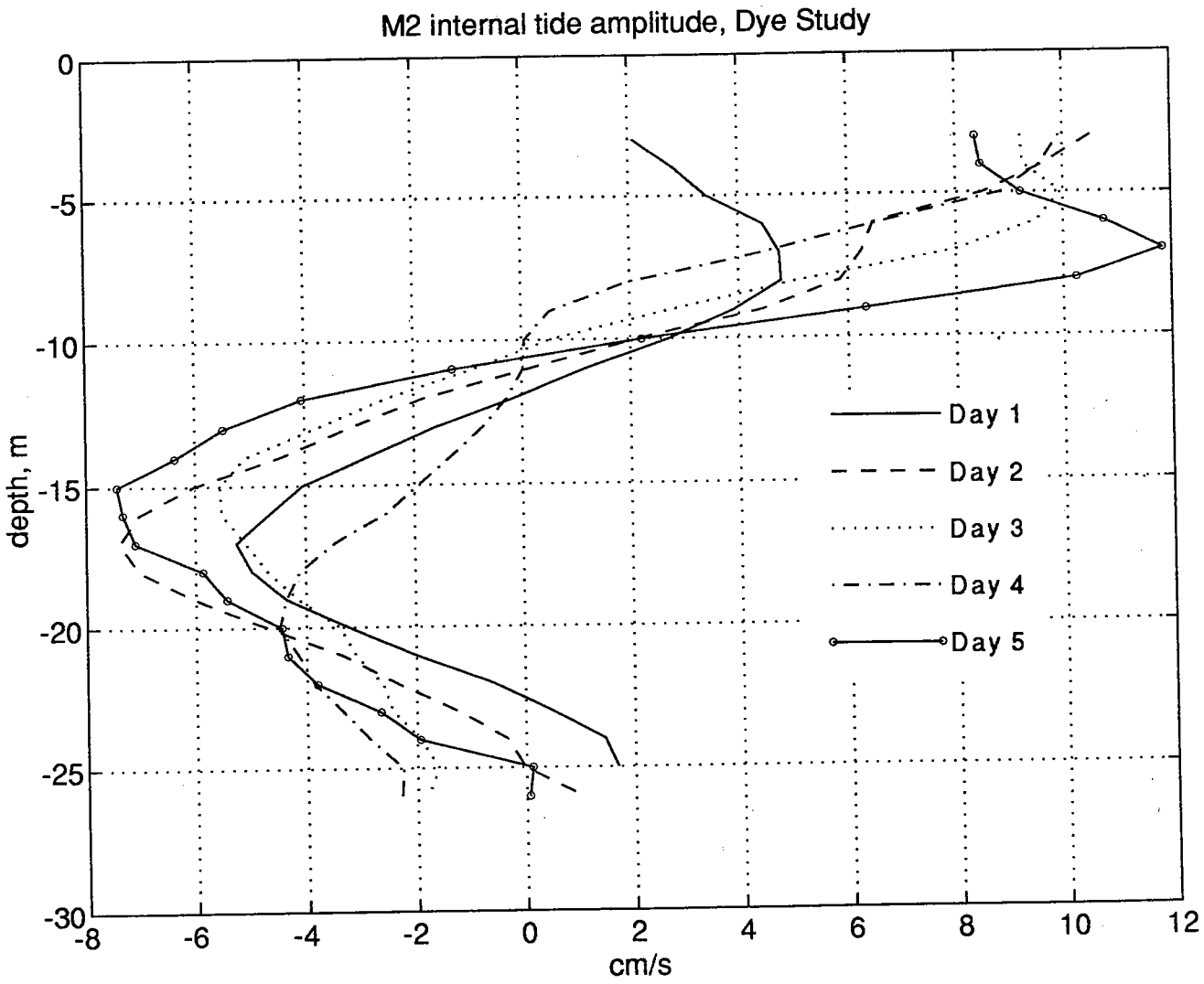

15. The vertical structure of the semidiurnal tidal amplitude, based on the ADCP data. Although the vertical structure is similar during the 5 days of observations, the phase and direction of the current varies by more than 90°, indicating highly variable forcing conditions. The extent to which the internal tides were locally vs. remotely forced was not determined.

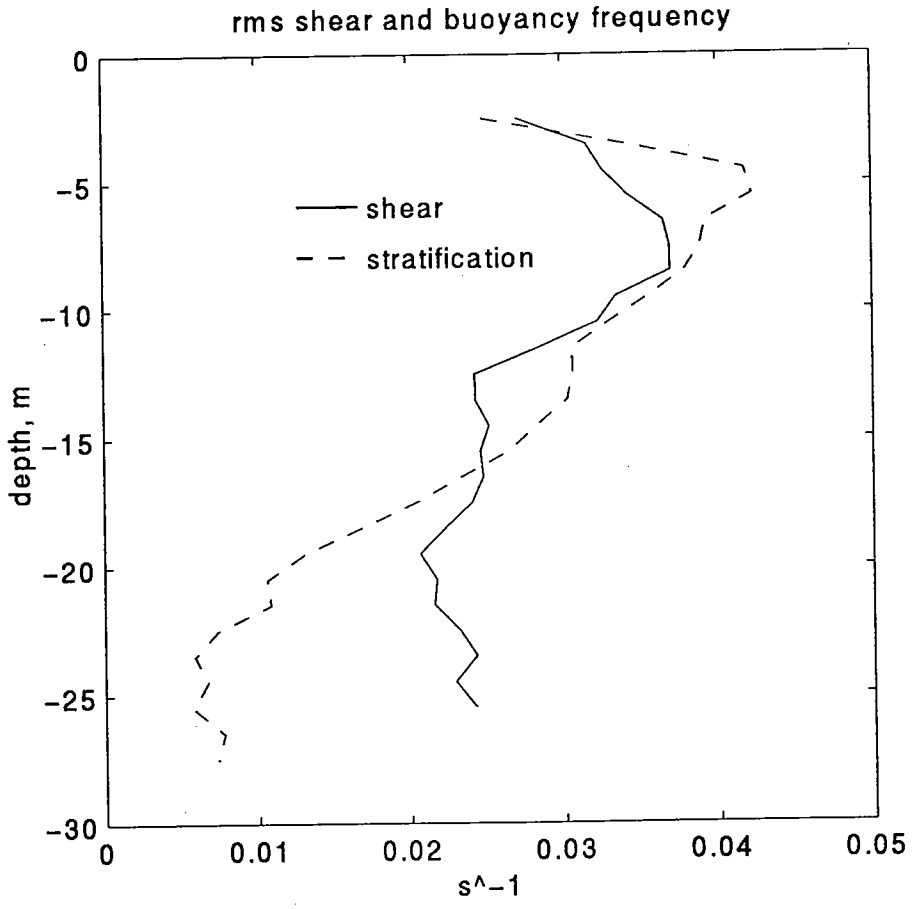

16. The rms magnitude of the shear and stratification (as buoyancy frequency) averaged over the 5 days of the dye study. Most of the shear is due to internal tidal fluctuations, with a minor contribution from the mean and high-frequency fluctuations.

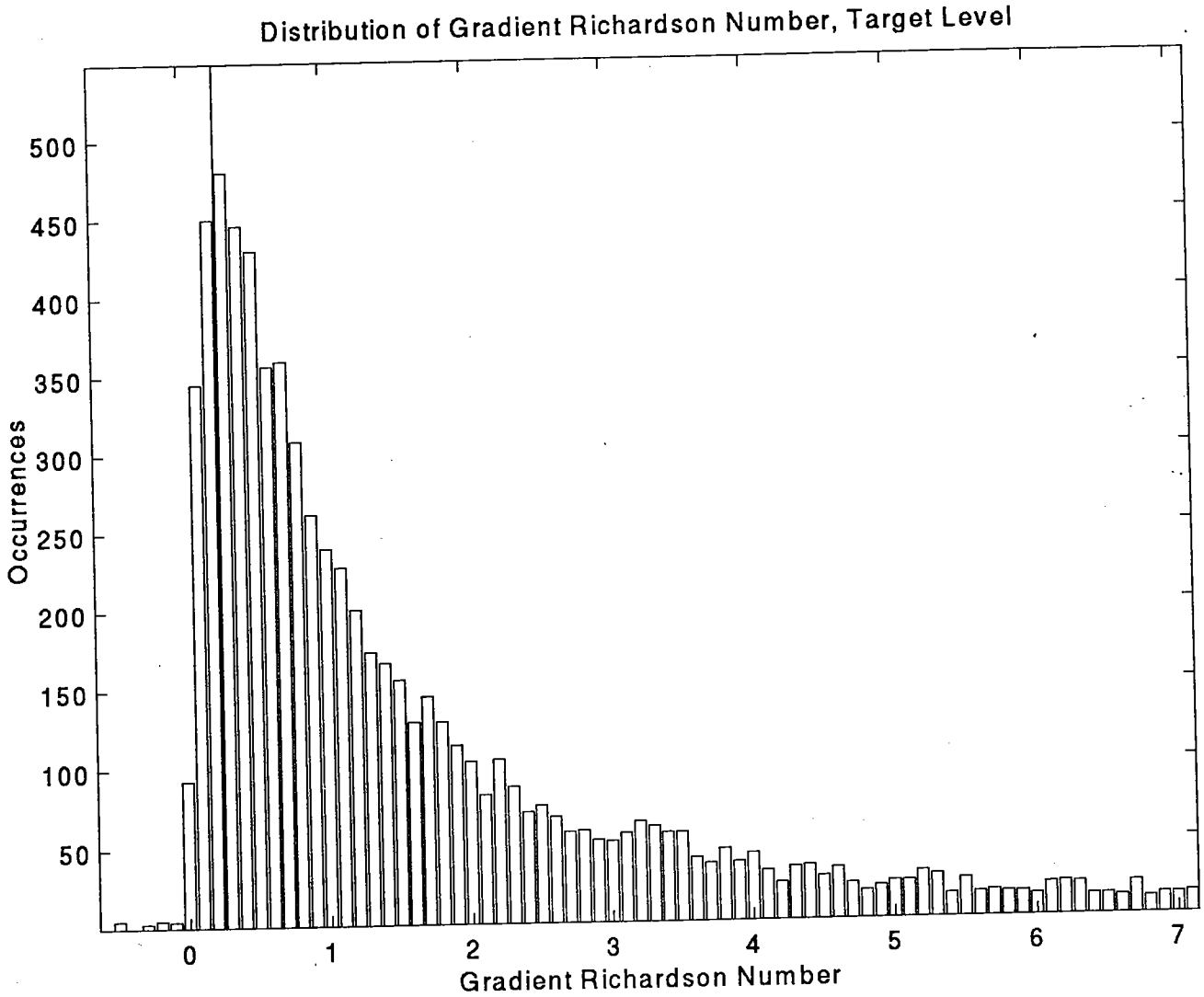

17. Histogram of the distribution of gradient Richardson number $Ri = N^2/S^2$, where N is the buoyancy frequency and S is the shear. Based on stability theory, $Ri = 0.25$ marks the threshold for shear instability. Approximately 10% of the measurements indicate unstable values. The vertical scale of these estimates is 1 m.

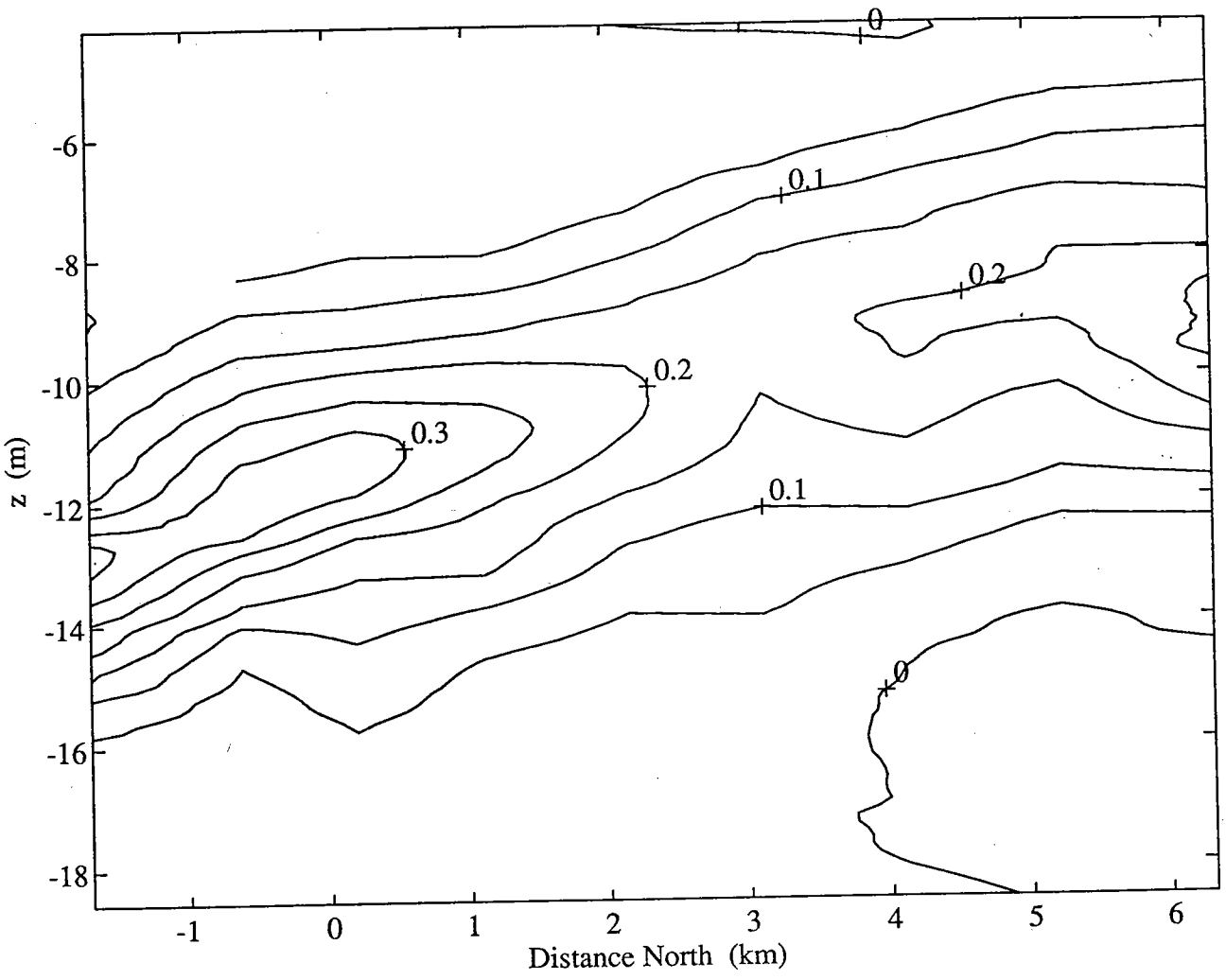

18. North–south section of E–W averaged dye concentration (ppb), based on 9 E–W crossings, 1-km apart. The vertical coordinate is based on a transformation from isothermal coordinates to depth based on the daily mean temperature gradient. The tilting of patch is due to vertical shear in the N–S direction.

Massachusetts Water Resources Authority
Charlestown Navy Yard
100 First Avenue
Boston, MA 02129
(617) 788-4719